

CASE FILE
COPY

NATIONAL ADVISORY COMMITTEE
FOR AERONAUTICS

TECHNICAL NOTE 2403

THE INDICIAL LIFT AND PITCHING MOMENT FOR A SINKING
OR PITCHING TWO-DIMENSIONAL WING FLYING
AT SUBSONIC OR SUPERSONIC SPEEDS

By Harvard Lomax, Max. A. Heaslet,
and Loma Sluder

Ames Aeronautical Laboratory
Moffett Field, Calif.



Washington

July 1951

NACA TN 2403

THE INDICIAL LIFT AND PITCHING MOMENT FOR A SINKING
OR PITCHING TWO-DIMENSIONAL WING FLYING
AT SUBSONIC OR SUPERSONIC SPEEDS

By Harvard Lomax, Max. A. Heaslet,
and Loma Sluder

SUMMARY

Solutions are presented for the lift and pitching moment on a two-dimensional flat plate undergoing a step variation in pitch or vertical displacement. Resulting indicial lift and pitching-moment curves are given for free-stream Mach numbers equal to 0, 0.8, 1.0, 1.2, and 2.0. Considerable use is made of the analogy between the boundary values for a two-dimensional wing in unsteady motion and those for a three-dimensional, lifting surface in steady motion. The incompressible, unsteady case, for which Wagner's classical treatment already exists, is shown to be analogous to a problem in slender wing theory.

INTRODUCTION

The response in lift for a two-dimensional airfoil that starts suddenly from rest and moves forward at a constant velocity in an incompressible fluid was studied originally by Wagner (reference 1). It is well known that such a response, referred to as the indicial lift due to angle of attack, can, by suitable superposition, be used to find the lift on a wing undergoing an arbitrary variation of angle of attack with time. In particular, Garrick (reference 2) showed that Wagner's results were consistent with those obtained by Theodorsen (reference 3) for a harmonically oscillating wing.

Subsequently, aerodynamicists have become interested in the effect of compressibility on the unsteady motion of a wing. Most of this interest, however, has been focused on the problem of wing flutter which involves harmonic motion. Hence, the analysis of the compressibility effects has usually commenced with the immediate assumption that the motion is harmonic. Such studies which, in general, can be considered as an extension of the work of Theodorsen, have been particularly successful in the case of supersonic flow (e.g., reference 4). In subsonic studies, however, these methods have proven to be somewhat cumbersome.

The purpose of this report is to calculate the effects of compressibility on the indicial responses. At supersonic speeds (e.g., reference 5) some of these indicial curves have been obtained. The material presented here, however, will provide a complete set of indicial responses ($c_{l\alpha}$, $c_{m\alpha}$, c_{lq} , c_{mq}) for supersonic speeds and, what is more important, will also provide these same responses for subsonic speeds; the particular case of a free-stream Mach number equal to 0.8 having been chosen for detailed consideration. Results are also presented for a wing traveling at the speed of sound.

The analysis required to formulate these indicial curves is based on the two-dimensional wave equation having boundary conditions specified over the plane in which the wing moves. The particular boundary-value problems involved are, in fact, completely analogous to certain three-dimensional, steady-state, supersonic, lifting-surface problems. The latter field has received much attention during the last few years and analytical techniques have been developed by means of which many supersonic lifting-surface problems have been solved. Because of the analogy, these techniques can be applied to the field of two-dimensional, unsteady flow. The analogy even extends to the point where a two-dimensional wing moving unsteadily in an incompressible field has for its analog a three-dimensional, lifting surface moving steadily in a compressible medium at the speed of sound. By means of this correspondence, Wagner's classical result can be rederived as a problem in slender-wing theory.

The part of the analysis pertaining to the response of an unsteady wing traveling at a subsonic speed is lengthy and somewhat tedious regardless of the method of approach. With the use of indicial functions, however, the calculations are reasonably straightforward, especially for Mach numbers around 0.8 to 1.0. Further, the use of indicial functions sheds considerable light on the manner in which Mach number variations affect the section aerodynamic characteristics.

LIST OF IMPORTANT SYMBOLS

a_0	velocity of sound in the free stream
c	chord of wing
c_l	section lift coefficient $\left(\frac{l}{q_0 c} \right)$
c_m	section moment coefficient $\left(\frac{m}{q_0 c^2} \right)$
$c_{l\alpha}$	indicial section lift coefficient due to angle-of-attack change (without pitching)

c_{lq}	indicial section lift coefficient due to pitching on a wing rotating about its leading edge
$c_{m\alpha}$	indicial section pitching-moment coefficient due to angle-of-attack change (without pitching) measured about the leading edge and considered positive when the trailing edge is forced down
c_{mq}	indicial section pitching-moment coefficient due to pitching measured about the leading edge for a wing rotating about its leading edge; considered positive when the trailing edge is forced down
$\left(c_{mq} \right)_{3/4}$	indicial section pitching-moment coefficient due to pitching measured about the leading edge for a wing rotating about its 3/4-chord point
l	section lift
m	section moment
M_0	flight Mach number
p	static pressure
Δp	$p_l - p_u$
q	$\frac{\rho c}{V_0}$
q_0	dynamic pressure $\left(\frac{1}{2} \rho_0 V_0^2 \right)$
r, s	oblique coordinates $\left(r = \frac{t-x}{\sqrt{2}}, s = \frac{t+x}{\sqrt{2}} \right)$
r_d	$\frac{s(1+M_0) - c\sqrt{2}}{1-M_0}$
t'	time
t	$a_0 t'$
t_0	$\frac{a_0 t'}{c} = \frac{t}{c}$
u, v, w	perturbation velocity components in the x, y, z directions, respectively
Δu	$u_1 - u_2$

V_0	flight velocity
x, y, z	Cartesian coordinates
x_0	$\frac{x}{c}$
α	angle of attack in radians
β	$\sqrt{ 1-M_0^2 }$
Γ	circulation strength
$\delta(t')$	Dirac δ function, normalized with respect to t' , thus
	$\int_{-\infty}^{\infty} \delta(t') dt' = 1$
$\delta(0)$	$\lim_{t' \rightarrow 0} \delta(t')$
θ	angle of pitch in radians
ρ_0	density in undisturbed air
ϕ	perturbation velocity potential

Subscripts

u	upper side of $z=0$ plane
l	lower side of $z=0$ plane
i	variable of integration
δ	part of a response multiplied by a δ function

METHOD

A basic linearized form of the partial differential equation which governs the flow field surrounding a thin wing moving through the air can be written in terms of the perturbation velocity potential, ϕ , as

$$\phi_{xx} + \phi_{yy} + \phi_{zz} = \frac{1}{a_0^2} \phi_{t't'} \quad (1)$$

where

x, y, z spatial coordinates

t' true time

a_0 speed of sound

Equation (1) is applicable when the fluid at infinity is at rest with respect to the x, y, z coordinate system and the wing or body traces certain space curves for which time is the parameter; moreover the perturbation velocity components $u=\phi_x$, $v=\phi_y$, $w=\phi_z$ must be small relative to the flight velocity V_0 of the wing.

In the following analysis a flat-plate wing moving in the $z=0$ plane away from the origin along the negative x axis will be studied. Since the variations in the flow along the span will be neglected and the slope of the stream lines at the wing surface will be taken as the ratio of w_u , the vertical induced velocity in the $z=0$ plane,¹ to V_0 , the constant forward velocity of the wing, the analysis is consistent with the assumptions of two-dimensional thin-airfoil theory. Hence, for the incompressible case, the partial differential equation reduces to

$$\phi_{xx} + \phi_{zz} = 0 \quad (2)$$

since the speed of sound is very large with respect to the velocity of the wing, and for the compressible case it reduces to

$$\phi_{xx} + \phi_{zz} = \phi_{tt} \quad (3)$$

where t equals $a_0 t'$.

The boundary conditions reduce to the specification of w_u over that portion of the xy plane occupied by the wing as time progresses.

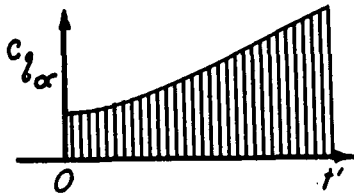
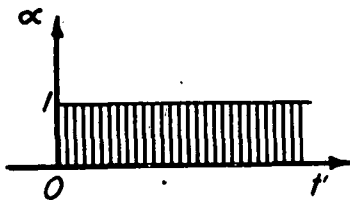
The solution in terms of ϕ can be converted into the loading coefficient by means of the equation

$$\frac{\Delta p}{q_0} = \frac{4}{V_0^2} \frac{\partial \phi}{\partial t'} = \frac{4}{V_0 M_0} \frac{\partial \phi}{\partial t} \quad (4)$$

The results for section lift and pitching moment can then be evaluated by appropriate integrations.

¹The subscript u indicates the value of w as z approaches zero from above. Since the discussion is limited to flat-plate surfaces without thickness, this is the same as the value of w obtained as z approaches zero from below, and thus w_u simply refers to the value of w in the $z=0$ plane.

Boundary Conditions for the Indicial Functions



(a)

The fundamental boundary-value problem to be considered in this report is the one generating the so-called indicial curves for loading, lift, and pitching moment. By definition, an indicial function is the response to a disturbance which is applied abruptly at time equals zero and is held constant thereafter; that is, a disturbance given by a step function. For example, if the angle of attack of a wing varies with time as shown in sketch (a), the resulting lift coefficient, also shown in sketch (a), is designated as the indicial lift coefficient due to angle of attack. Four such indicial functions will be evaluated,

namely:

- $c_{l\alpha}$ the indicial section lift coefficient due to angle-of-attack change (without pitching)
- $c_{m\alpha}$ the indicial section pitching-moment coefficient due to angle-of-attack change (without pitching) measured about the leading edge and considered positive when the trailing edge is forced down
- c_{lq} the indicial section lift coefficient due to pitching on a wing rotating about its leading edge
- c_{mq} the indicial section pitching-moment coefficient due to pitching measured about the leading edge for a wing rotating about its leading edge and considered positive when the trailing edge is forced down

The equations which transform these functions to those for a wing pitching about a point a distance ac back from the leading edge and having its moment center a distance bc back from the leading edge are simply

$$c_{l\alpha} = c_{l\alpha}$$

$$c_{m\alpha} = c_{m\alpha}' + b c_{l\alpha}$$

$$c_{l_q} = c_{l_q}' - a c_{l\alpha}$$

$$c_{m_q} = c_{m_q}' + b c_{l_q}' - a c_{m\alpha}' - ab c_{l\alpha}$$

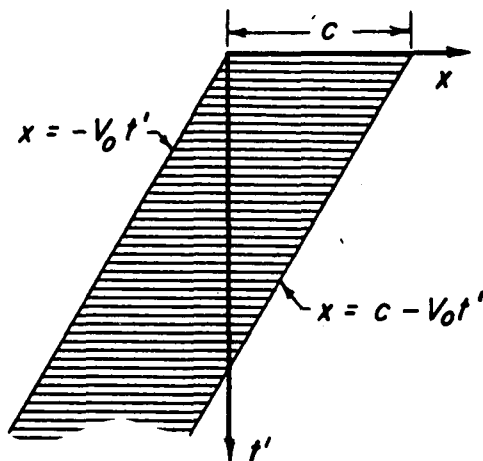
The boundary condition which applies to the indicial functions due to angle of attack is simply that

$$w_u = -V_0\alpha \tag{5}$$

over a certain planar area in xzt space representing the area occupied by the wing, and elsewhere pressure is continuous. For a wing of chord length c , this area, shown shaded in sketch (b), is bounded by the traces of the leading and trailing edges, $x = -V_0t'$ and $x = c - V_0t'$, and the line along which the motion started (i. e., the x axis).

In the case of the indicial function due to pitch for a wing rotating about its leading edge, the boundary condition requires that the upwash be given by the expression

$$w_u = -(x + V_0t') \dot{\theta} \tag{6}$$



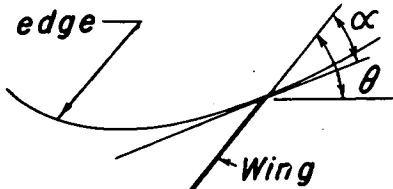
(b)

over the same region in the xt plane as for the angle of attack case and, again, that pressure be continuous elsewhere. The angle of pitch, θ , is taken as positive when the trailing edge is lower than the leading edge, and $\dot{\theta}$ is the time derivative, $d\theta/dt'$, positive when the trailing edge is falling with reference to the leading edge.

Direction of wing motion



Flight path of leading edge

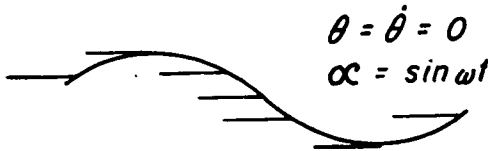


Flight path of arbitrary point

(c)

The difference between θ and α is illustrated in sketch (c). The angle of attack α is the angle between the flat wing surface and the tangent to the flight path of the leading edge. The angle θ is the angle between the flat wing surface and the horizontal. Sketch (d) shows a wing undergoing a sinusoidal angle-of-attack variation with a zero angle of pitch throughout. For convenience and in order to distinguish from the pitching wing, such a wing will be referred to as a sinking wing. Sketch (e) shows a wing undergoing a sinusoidal angle-of-pitch variation taken about the leading edge at a constant (zero) angle of attack.

The variable q to which the lift and pitching-moment coefficients of the pitching wing are referred is equal to $\dot{\theta}c/V_0$, a dimensionless form of expression for rate of pitch.



(d)

Adaptation of the Indicial Functions to Maneuvers

When the wing is undergoing a maneuver in which α and θ make small but arbitrary deviations from zero, the boundary condition in the region of the xt plane traversed by the wing becomes

$$w_u = -V_0 \alpha - (x + V_0 t') \dot{\theta} \quad (7)$$

Since the theory is linear, the lift and moment on the wing are calculated from the indicial functions by the principle of superposition. For example, the lift and pitching-moment coefficients developed by an arbitrary variation of α and θ are

$$\left. \begin{aligned} c_l &= \frac{d}{dt'} \int_0^{t'} \left[c_{l_\alpha} (t' - t_1') \alpha(t_1') dt_1' + c_{l_q} (t' - t_1') q(t_1') dt_1' \right] \\ c_m &= \frac{d}{dt'} \int_0^{t'} \left[c_{m_\alpha} (t' - t_1') \alpha(t_1') dt_1' + c_{m_q} (t' - t_1') q(t_1') dt_1' \right] \end{aligned} \right\} (8)$$

Equation (8) is derived for an angle-of-attack variation measured with respect to the flight path of the leading edge and the primes on the derivatives indicate that the wing is pitching about and the moments are measured with respect to the wing leading edge. If the angle of attack is measured with respect to the flight path of some other point on the wing (as, for example, the center of gravity), then it can be shown for small deflections that

$$\alpha = \alpha_1 - \frac{c\xi \dot{\theta}_1}{V_0}$$

$$\theta = \theta_1$$

where α_1 and θ_1 are the angles measured with respect to the new flight path and $c\xi$ is the distance from the leading edge to the new reference point. (See sketch (c).) The total value of the section lift and pitching-moment coefficients for an arbitrary variation of α_1 and θ_1 would be

$$c_l = \frac{d}{dt'} \int_0^{t'} \left\{ c_{l\alpha}(t'-t_1') \left[\alpha_1(t_1') - \xi q_1(t_1') \right] + c_{lq}(t'-t_1') q_1(t_1') \right\} dt_1'$$

$$c_m' = \frac{d}{dt'} \int_0^{t'} \left\{ c_{m\alpha}'(t'-t_1') \left[\alpha_1(t_1') - \xi q_1(t_1') \right] + c_{mq}'(t'-t_1') q_1(t_1') \right\} dt_1'$$

Adaptation of the Indicial Functions to Flutter Derivatives

The notation adopted in this report does not coincide with the usual notation used in the study of fluttering wings; however, it should be sufficient to relate the present notation to the one used in reference 4. Thus, the values of the terms L_1, L_2, L_3', L_4' and M_1', M_2', M_3', M_4' used in reference 4 can be evaluated as follows:

$$\left. \begin{aligned} L_1 + iL_2 &= \frac{ie^{-i\omega t'}}{4k} \lim_{t' \rightarrow \infty} \frac{d}{dt'} \int_0^{t'} c_{l\alpha}(t'-t_1') e^{i\omega t_1'} dt_1' \\ M_1' + iM_2' &= \frac{ie^{-i\omega t'}}{2k} \lim_{t' \rightarrow \infty} \frac{d}{dt'} \int_0^{t'} c_{m\alpha}'(t'-t_1') e^{i\omega t_1'} dt_1' \end{aligned} \right\} (9)$$

$$\left. \begin{aligned} L_3' + iL_4' &= \frac{e^{-i\omega t'}}{4k^2} \lim_{t' \rightarrow \infty} \frac{d}{dt'} \int_0^{t'} \left[c_{l\alpha}(t'-t_1') + i\omega c_{lq}(t'-t_1') \right] e^{i\omega t_1'} dt_1' \\ M_3' + iM_4' &= \frac{e^{-i\omega t'}}{2k^2} \lim_{t' \rightarrow \infty} \frac{d}{dt'} \int_0^{t'} \left[c_{m\alpha}(t'-t_1') + i\omega c_{mq}(t'-t_1') \right] e^{i\omega t_1'} dt_1' \end{aligned} \right\} (9)$$

THE SOLUTION FOR THE INDICIAL FUNCTIONS

The boundary conditions which represent a wing undergoing a sudden jump in pitching velocity or angle of attack have been discussed and presented in equations (5) and (6). Their application to wings flying at several Mach numbers will now be presented. The incompressible case will first be discussed, and then the cases in which M_0 equals 0.8, 1.0, 1.2, and 2.0 will be considered.

Incompressible Case, $M_0 = 0$

The solution for the incompressible case is applicable when the forward speed of the wing is small compared with the speed of sound so that the ratio V_0/a_0 can be neglected in comparison to unity. The basic partial differential equation governing the flow field was presented in equation (2) as

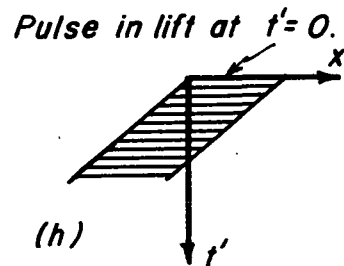
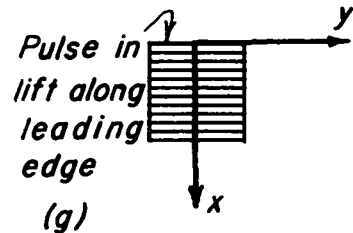
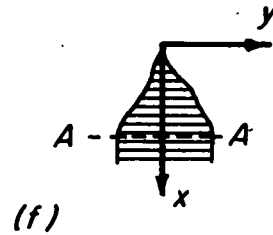
$$\Phi_{xx} + \Phi_{zz} = 0$$

subject to the boundary conditions discussed, and the equation for the loading coefficient was given in equation (4) as

$$\Delta p/q_0 = \frac{4}{V_0^2} \frac{\partial \Phi}{\partial t'}$$

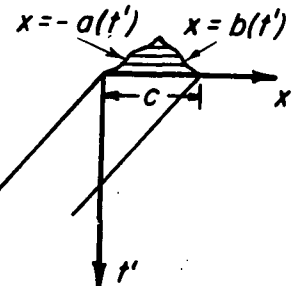
This boundary-value problem corresponds precisely to that which is studied in three-dimensional, steady-state, lifting-surface theory under the classification "slender-wing theory." (See references 6 and 7.) Such an analogy is useful since well-established concepts in one theory can be immediately carried over into the other. (It should be re-emphasized, perhaps, that the subsequent treatment of the incompressible case is not intended to be an improvement on Wagner's original derivation but rather it is a rederivation along lines that will be used later in the analysis of the compressible cases.)

The initial pulse.— The first analogy with slender-wing theory which will be used concerns the initial pulses that occur in the values of lift and pitching moment. It is a well-known result (reference 6) that the total lift, as given by slender-wing theory, on the wing shown in sketch (f) is a function only of the maximum span and the value of w_u along the section of maximum span (section AA). It is, therefore, independent of the wing twist and leading-edge shape ahead of section AA. This concept has been extended in slender-wing theory to the extreme case shown in sketch (g) of a rectangular wing. The lift on such a wing is concentrated entirely along the leading edge and is a function only of the span of that edge and the value of w_u there. By the analogy existing between the two theories, therefore, it is evident that the solution to the indicial problems in two-dimensional, incompressible, unsteady flow (sketch (h)) will contain a pulse at $t'=0$.



The evaluation of this pulse will be treated briefly. A solution to equation (2) for the vertical induced velocity in the $z=0$ plane can be written in terms of the jump in u across the $z=0$ plane (see reference 7), thus, for the shaded area in sketch (i) this is

$$w_u(x) = -\frac{1}{2\pi} \int_{-a}^b \frac{\Delta u(x_1)}{x-x_1} dx_1 \quad (10)$$



The general inversion of equation (10) can be written

$$\Delta u(x) = \frac{A}{\pi \sqrt{(x+a)(b-x)}} + \frac{2}{\pi \sqrt{(x+a)(b-x)}} \int_{-a}^b \frac{w_u(x_1)}{x-x_1} \sqrt{(x_1+a)(b-x_1)} dx_1 \quad (11)$$

where

$$A = \int_{-a}^b \Delta u dx$$

In the present case A is zero, since $\Delta\phi$ is zero at $x=-a$ and $x=b$, and an integration of both sides of equation (11) with respect to x between the limits b and x gives

$$\Delta\phi(t', x) = -\frac{4}{\pi} \int_{-a}^b w(t', x_1) \ln \frac{\sqrt{(b-x_1)(a+x)} + \sqrt{(a+x_1)(b-x)}}{\sqrt{(x-x_1)(a+b)}} dx_1$$

Adoption of the notation

$$v(t', x_1) + \text{constant} = \int w(t', x_1) dx_1$$

and integration by parts leads to the equation²

$$\Delta\phi = -\frac{2\sqrt{(b-x)(a+x)}}{\pi} \int_{-a}^b \frac{v(t', x_1) dx_1}{(x-x_1)\sqrt{(b-x_1)(a+x_1)}} \quad (12)$$

The loading can now be determined by using equation (4). If the shaded area in sketch (i) is allowed to vanish, all the loading accumulates along the x axis in the region $0 \leq x \leq c$. Therefore, the integral of the loading with respect to t' over the shaded portion must be considered. The final result for the pulse loading $(\Delta p/q_0)_\delta$ at $t'=0$ can be expressed in terms of the δ function (see list of symbols) as

$$\left(\frac{\Delta p}{q_0}\right)_\delta = -\frac{4\delta(0)}{\pi V_0^2} \sqrt{(c-x)x} \int_0^c \frac{v(0, x_1) dx_1}{(x-x_1)\sqrt{(c-x_1)x_1}} \quad (13)$$

The boundary conditions for the sinking and pitching wing given by equations (5) and (6), when inserted into equation (13), yield

$$\left. \begin{aligned} \left(\frac{\Delta p}{q_0 \alpha}\right)_\delta &= \frac{4\delta(0)}{V_0} \sqrt{(c-x)x} \\ \left(\frac{\Delta p}{q_0 \theta}\right)_\delta &= \frac{(c+2x)\delta(0)}{V_0^2} \sqrt{(c-x)x} \end{aligned} \right\} \quad (14)$$

²The constant gives zero when placed in equation (12), provided $b > x > -a$.

After integration, the pulse values for lift and pitching moment may also be obtained. Hence,

$$\left. \begin{aligned}
 \left(c_{l\alpha} \right)_{\delta} &= \frac{\pi c}{2V_0} \delta(0) \\
 \left(c_{m\alpha}' \right)_{\delta} &= -\frac{\pi c}{4V_0} \delta(0) \\
 \left(c_{lq}' \right)_{\delta} &= \frac{\pi c}{4V_0} \delta(0) \\
 \left(c_{mq}' \right)_{\delta} &= -\frac{9}{64} \frac{\pi c}{V_0} \delta(0)
 \end{aligned} \right\} \quad (15)$$

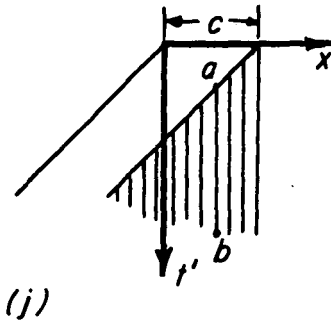
where the primes indicate that the wings are pitching about and the moments are measured about the leading edge. These expressions may be inserted in equations (8) and (9) and, since the integrand becomes zero everywhere except at the point $t_1' = t'$, the expressions for the lift and pitching-moment coefficient developed by an arbitrary variation of α and θ with time are

$$c_l = \frac{\pi c}{2V_0} \dot{\alpha} + \frac{\pi c^2}{4V_0^2} \ddot{\theta}$$

$$c_m' = -\frac{\pi c}{4V_0} \dot{\alpha} - \frac{9}{64} \frac{\pi c^2}{V_0^2} \ddot{\theta}$$

The variation for $t' > 0$.—The integral equation (10) is still perfectly valid when applied to the flow field for $t' > 0$. It is convenient to rewrite the equation in this case, however, so that the effects of the vorticity on the wing and in the wake are separated. Thus,

$$w_u = -\frac{1}{2\pi} \int_{-V_0 t'}^{c-V_0 t'} \frac{\Delta u(t', x_1)}{x-x_1} dx_1 - \frac{1}{2\pi} \int_{c-V_0 t'}^c \frac{\Delta u^*(x_1)}{x-x_1} dx_1 \quad (16)$$



where $\Delta u^*(x_1)$ is the value of Δu in the starting vortex wake. It is independent of t' since its value at all points along the line ab in sketch (j) is the same as at the point a .

A reduction of equation (16) can be obtained for the case of the sinking wing, where $w_u = -V_0\alpha$, by using the inversion given by equation (11). Thus,

$$\pi\Delta u(t', x) \sqrt{(x+V_0t')(c-V_0t'-x)} = A - \pi(2x+2V_0t'-c) V_0\alpha + \int_{c-V_0t'}^c \Delta u^*(x_1) \left[1 + \frac{\sqrt{(x_1+V_0t')(x-c+V_0t')}}{(x-x_1)} \right] dx_1$$

Since A is given by the relation

$$A = \int_{-V_0t'}^{c-V_0t'} \Delta u(t', x_1) dx_1 = - \int_{c-V_0t'}^c \Delta u^*(x_1) dx_1$$

it follows that

$$\Delta u(t', x) = - \frac{V_0\alpha(2x+2V_0t'-c)}{\sqrt{(x+V_0t')(c-V_0t'-x)}} + \frac{1}{\pi \sqrt{(x+V_0t')(c-V_0t'-x)}}$$

$$\int_{c-V_0t'}^c \frac{\Delta u^*(x_1)}{x-x_1} \sqrt{(x_1+V_0t')(x_1-c+V_0t')} dx_1 \quad (17)$$

According to the Kutta condition $\Delta u(t', x)$ vanishes as x approaches $c-V_0t'$; the integral equation for $\Delta u^*(x_1)$ thus becomes

$$V_0\alpha = - \frac{1}{\pi c} \int_{c-V_0t'}^c \Delta u^*(x_1) \sqrt{\frac{x_1+V_0t'}{x_1-c+V_0t'}} dx_1 \quad (18)$$

which was derived and studied originally by Wagner (reference 1).

The section lift and pitching moment can be derived in terms of $\Delta u^*(x_1)$ in the following manner. By definition, the section lift l is

$$l = \frac{1}{2} \rho_0 V_0^2 \int_{-V_0 t'}^{c-V_0 t'} \frac{\Delta p}{q_0} dx = \rho_0 \int_{-V_0 t'}^{c-V_0 t'} \frac{\partial \Delta \phi}{\partial t'} dx \quad (19)$$

Since the value of $\Delta \phi$ is zero at the leading edge and at the trailing edge is equal to the total circulation Γ , two alternative forms for the lift can be written

$$l = \rho_0 V_0 \Gamma + \rho_0 \frac{\partial}{\partial t'} \int_{-V_0 t'}^{c-V_0 t'} \Delta \phi(t', x) dx \quad (20)$$

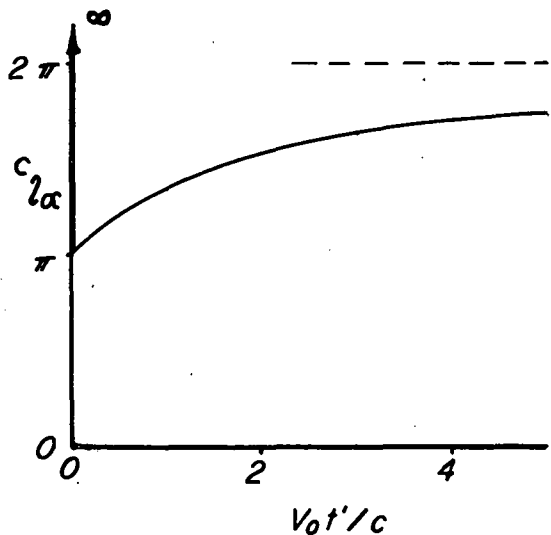
and

$$l = \rho_0 (c-V_0 t') \frac{d\Gamma}{dt'} - \rho_0 \frac{\partial}{\partial t'} \int_{-V_0 t'}^{c-V_0 t'} x \Delta u(t', x) dx \quad (21)$$

By substituting equation (17) into (21) and integrating, it can be shown that

$$l = \pi \rho_0 c V_0^2 \alpha + \frac{\rho_0 c V_0}{2} \int_{c-V_0 t'}^c \frac{\Delta u^*(x_1)}{\sqrt{(x_1+V_0 t')(x_1-c+V_0 t')}} dx_1 \quad (22)$$

Since the value of $\Delta u^*(x_1)$ has been determined by Wagner, equation (22) represents a solution for the section lift. A plot of its variation in coefficient form is shown in sketch (k). Initially there is the pulse having an intensity defined by equation (15). After the pulse at $t'=0$, the value of the section lift coefficient starts at one-half its asymptotic value. It then increases, slowly approaching its asymptote of 2π .



(k)

By definition, the pitching moment can be written

$$\begin{aligned}
 m &= -\frac{1}{2} \rho_0 V_0^2 \int_{-V_0 t'}^{c-V_0 t'} (V_0 t' + x) \frac{\Delta p}{q_0} dx \\
 &= -\rho_0 \int_{-V_0 t'}^{c-V_0 t'} (V_0 t' + x) \frac{\partial \Delta \phi}{\partial t'} dx
 \end{aligned}
 \tag{23}$$

where the moment is taken about the leading edge and is positive when the trailing edge is forced down. A development, similar to the one given for the lift, gives

$$m = -\frac{c}{4} l \tag{24}$$

This result, that for $t > 0$ the indicial center of pressure remains constant at the quarter chord throughout the motion, is classical.

If the boundary condition for a pitching wing, $w_u = -(x+V_0 t') \dot{\theta}$, is substituted into equation (16) and the inversion given by equation (11) is again used, it can be shown in the same manner used in the derivation of equation (18) that for $x = c - V_0 t'$ the relation

$$\frac{3}{4} c^2 \dot{\theta} = -\frac{1}{\pi} \int_{c-V_0 t'}^c \Delta u^*(x_1) \sqrt{\frac{x_1+V_0 t'}{x_1-c+V_0 t'}} dx_1$$

applies. This integral equation applies to a wing pitching about its leading edge. If, instead, the wing is pitching about the three-quarter-chord position, an essential simplification is achieved. In this latter case, downwash is given by the expression

$$w_u = -\dot{\theta} \left(x + V_0 t' - \frac{3}{4} c \right) \tag{25}$$

and the resulting integral equation becomes

$$0 = \int_{c-V_0 t'}^c \Delta u_3^*(x_1) \sqrt{\frac{x_1+V_0 t'}{x_1-c+V_0 t'}} dx_1 \tag{26}$$

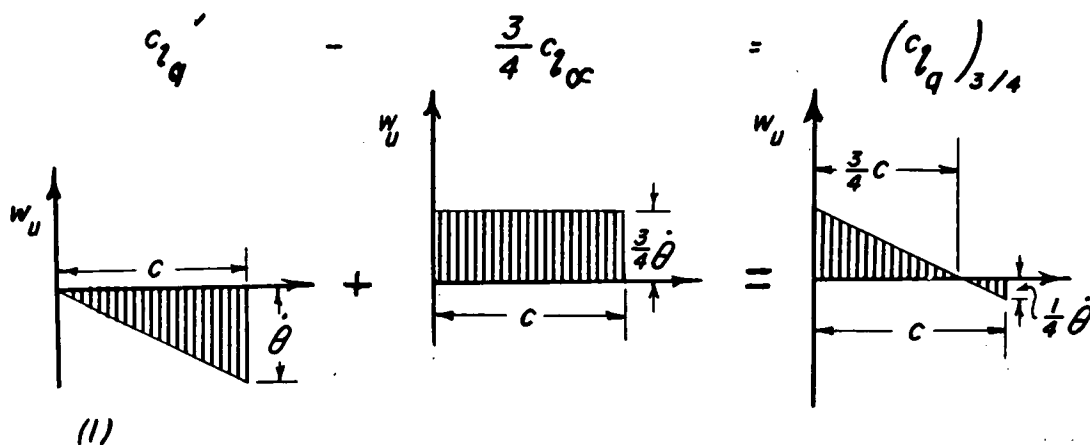
where $\Delta u_3^*(x_1)$ represents the vorticity in the wake following such a motion. The solution to equation (26) is simply

$$\Delta u_3^*(x_1) = 0 \tag{27}$$

From equation (27) it follows that the total indicial lift for $t' > 0$ on a wing pitching about the three-quarter chord point is zero, and that the wing wake is free of vorticity. Further, it can be shown that the total indicial pitching moment (still measured about the leading edge) is

$$m = -\frac{\rho \pi c^3}{16} V_0 \dot{\theta} \tag{28}$$

The transfer of equations (27) and (28) back to the case in which the wing is pitching about its leading edge can be readily accomplished by means of the boundary conditions shown in sketch (1). Hence, if



$(c_{lq})_{3/4}$ refers to the lift coefficient on a wing pitching about the three-quarter chord point and $(c_{mq}')_{3/4}$ refers to the pitching-moment coefficient measured about the leading edge of a wing pitching about the three-quarter chord point, then

$$\left. \begin{aligned} (c_{lq})_{3/4} &= c_{lq}' - \frac{3}{4} c_{l\alpha} \\ (c_{mq}')_{3/4} &= c_{mq}' - \frac{3}{4} c_{m\alpha}' \end{aligned} \right\} \tag{29}$$

By means of equations (24) and (29) the expressions for the three indicial functions, $c_{m\alpha}'$, c_{lq}' , and c_{mq}' can all be written in terms of the indicial lift function for $t > 0$. Hence,

$$\left. \begin{aligned} c_{m\alpha}' &= -\frac{1}{4} c_{l\alpha} \\ c_{lq}' &= \frac{3}{4} c_{l\alpha} \\ c_{mq}' &= -\frac{3}{16} c_{l\alpha} - \frac{\pi}{8} \end{aligned} \right\} \quad (30)$$

The variations of the four indicial functions are shown in figure 1. For values of $V_0 t'/c$ larger than those shown in the figure the approximate equation suggested in reference 2 can be used, namely,

$$c_{l\alpha} = 2\pi \left[1 - \frac{1}{2 + (V_0 t'/c)} \right]$$

This alternative result has, according to reference 2, an error of 2 percent or less for the entire range of time from $0+$ to infinity.

Subsonic Case, $M_0 = 0.8$

When the Mach number is no longer small, the analysis in the preceding section must be modified. As an example of this modification, the calculations for a wing traveling at a Mach number equal to 0.8 will be carried out in detail.

Equation (3) presents the basic partial differential equation of the flow field, and equation (4) gives the expression for the loading coefficient. The analogy which existed in the incompressible case between the theory for the unsteady, two-dimensional wing and slender-wing theory exists in this case between the theory for the unsteady, two-dimensional wing and the theory for a steady-state, three-dimensional wing traveling at a supersonic speed. Thus, in the three-dimensional, steady-state case the partial differential equation governing the flow is

$$\Phi_{yy} + \Phi_{zz} = \beta^2 \Phi_{xx} \quad (31)$$

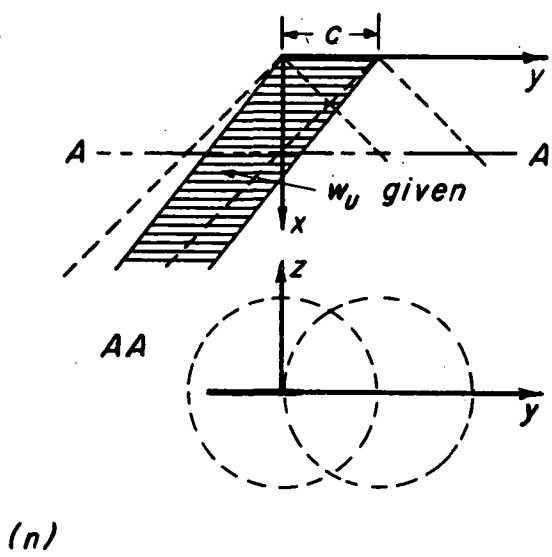
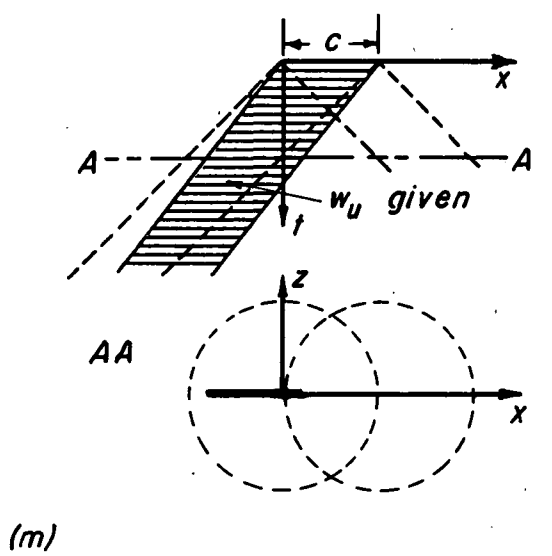
and the equation for the loading coefficient is

$$\frac{\Delta p}{q} = \frac{4}{V_0} \frac{\partial \phi}{\partial x} \tag{32}$$

The boundary conditions are in both cases that ϕ_z is given over a portion of the $z=0$ plane. It is evident by a comparison of equations (3) and (31) and equations (4) and (32) that results from the three-dimensional, supersonic, steady-state study (hereinafter referred to as the steady-state case) can be transferred to the two-dimensional, unsteady study (hereinafter referred to as the unsteady case) simply by replacing x , y , and β in the former case by t , x , and l , respectively, and by dividing the result for the loading coefficient by M_0 .

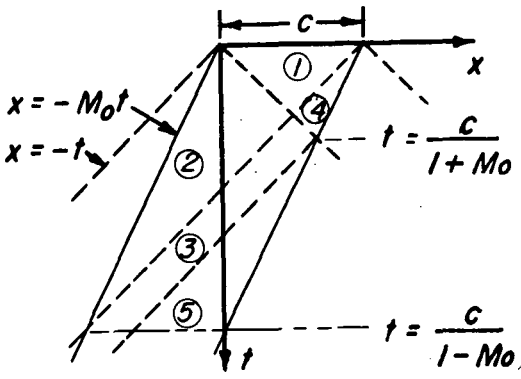
The analog to the boundary condition for the problem of finding the indicial loading on a two dimensional wing flying at a Mach number equal to 0.8 (sketch (m)) is the boundary condition for the problem of finding the loading on a constant-chord, swept-forward wing tip with a subsonic trailing edge such as that shown in sketch (n). The Mach cones in the steady-state case, traces of which are shown as dotted lines in sketch (n), become, in the unsteady-state analog, the locus of the sound waves which started at $t=0$ from the leading and trailing edges of the two-dimensional wing (sketch (m)). Finally, the analog in the steady-state field of the unsteady wing would be a flat plate for the unsteady sinking wing and a plate with a linear variation of twist for the unsteady pitching wing.

A detailed analysis of an unsteady, two-dimensional wing flying at a Mach number equal to 0.8 will be presented. Just as in the section on incompressible flow, the study will be divided into two parts. In cases for which $M_0 \neq 0$, however, the indicial functions contain no pulse at $t=0$. Hence, the first part



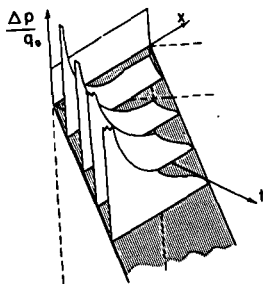
of the $M_0=0.8$ study will be concerned with the behavior of the indicial functions in an interval for which t is small but finite (actually $0 \leq t \leq 5c$) and the second part, with their asymptotic behavior.

The early stage.— The analog which exists between the steady-state and unsteady cases may be utilized to great advantage since the large number of special methods and techniques developed for the solution of problems in the former case may be applied to the solution of the analogous problems in the latter field. In this manner an exact solution for the loading over the five regions shown in sketch (o) may be obtained for both the sinking and the pitching wing in an unsteady flow field by the use of methods such



(o)

regions shown in sketch (o) on both the sinking and pitching wings is outlined in appendix A. Plots of the loading on a sinking wing are shown in sketch (p) and, in more detail, together with the loading on a pitching wing, in figure 2. At $t_0=0$ the loading is constant,³ and as time increases the loading-coefficient curve approaches the familiar two-dimensional, steady-state shape given, for the sinking wing, by the equation



(p)

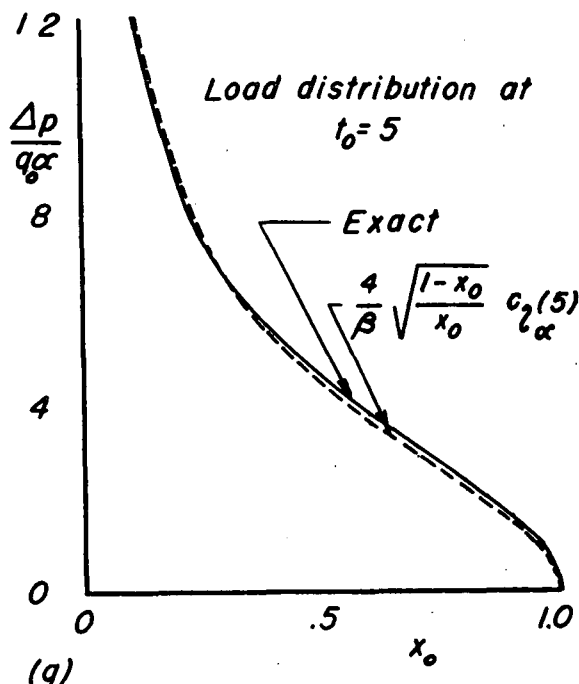
as those presented in reference 8. Solutions for larger values of time could also be obtained, but the labor involved in calculating such cases becomes prohibitive and, as will be shown later, approximate methods can be developed which extend the solutions for the indicial lift and pitching-moment curves to their asymptotic values.

The analysis used to calculate the loading in terms of $x_0 = x/c$ and $t_0 = t/c$ over the five

$$\frac{\Delta p}{q_\infty} = \frac{4\alpha}{\beta} \sqrt{\frac{c-x}{x}} \quad (33)$$

³The result that the initial shape of the load distribution is the same as the shape of the given curve for w_u also applies to all three-dimensional wings of arbitrary plan forms traveling at subsonic or supersonic Mach numbers.

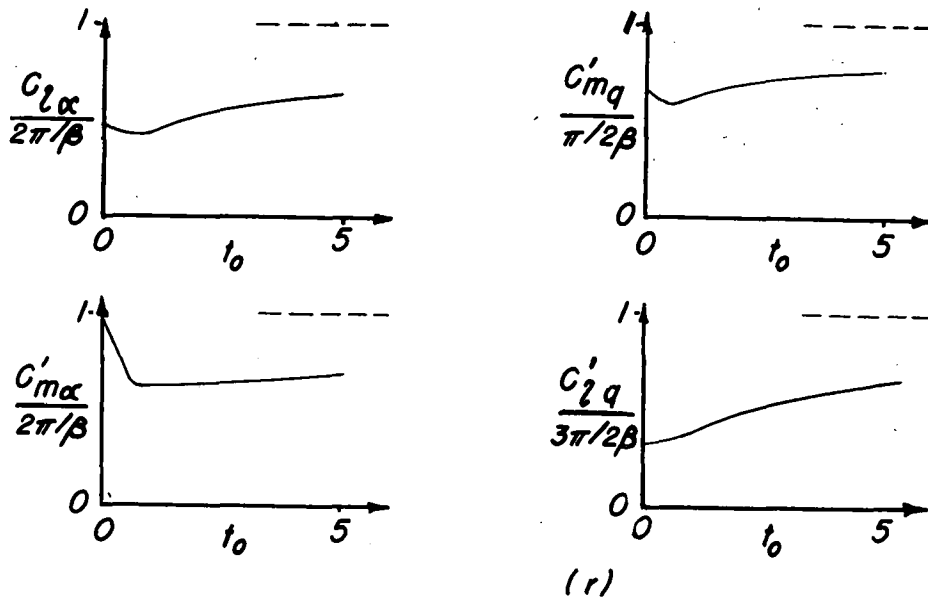
where x is the distance from the leading edge which is at the point $x=0$. Sketch (q) shows that the distribution at $t_0 = t/c = 1/(1-M_0) = 5$ is already essentially the same distribution as that obtained at $t_0=\infty$ (i.e., the agreement is good with the curve produced by multiplying the right side of equation (33) by a constant factor).⁴ The use of this fact simplifies subsequent analysis concerning the asymptotic behavior of the indicial lift curve.



The indicial lift and pitching-moment functions were also calculated (see appendix A) in the range $0 \leq t_0 \leq 1/(1-M_0)$. Their variation in this interval is shown in sketch (r) for $M_0 = 0.8$. It is evident that the calculations must be extended beyond the point $t_0=5$ since the asymptotic values are not yet even closely approached.

Before studying the nature of these curves for large values of t_0 , however, it is useful to examine them with reference to the discussion in the previous section on incompressible flow. For example, it was pointed out that the indicial center of pressure on the sinking wing remained at the quarter-chord point for $t' > 0$. It is, therefore, pertinent to consider the location of the center of pressure on the sinking wing when $M_0 = 0.8$. By means of the curves given for $c_{l\alpha}$ and $c_{m\alpha}'$ and by the relationship

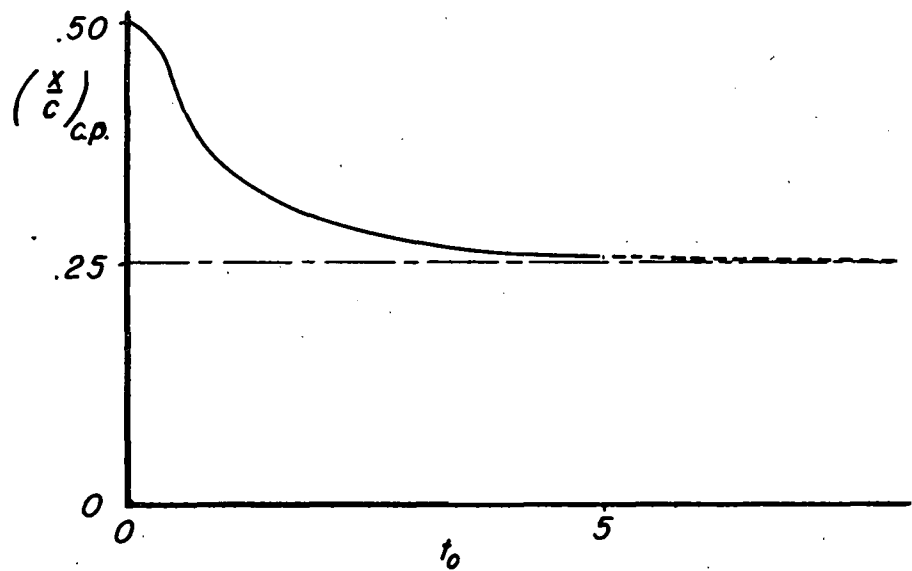
⁴A similar result was noted in the study of the load distribution on swept-back wings with subsonic leading edges (reference 9).



(r)

$$c_{m\alpha}' = - (x/c)_{c.p.} c_{l\alpha}$$

the variation of $(x/c)_{c.p.}$ is easily evaluated ($(x/c)_{c.p.}$ is the distance between the leading edge and the center of pressure divided by the total wing chord). This variation is shown in sketch (s). It is

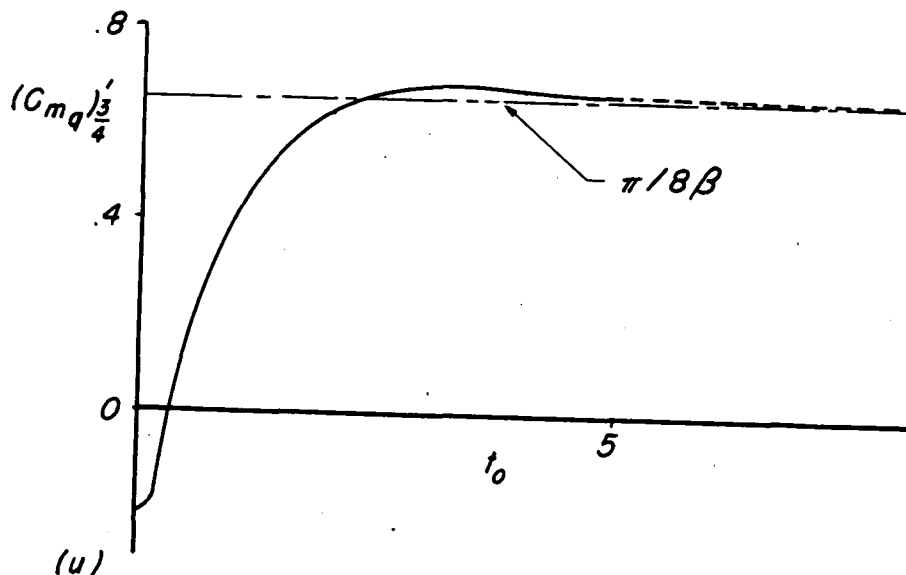
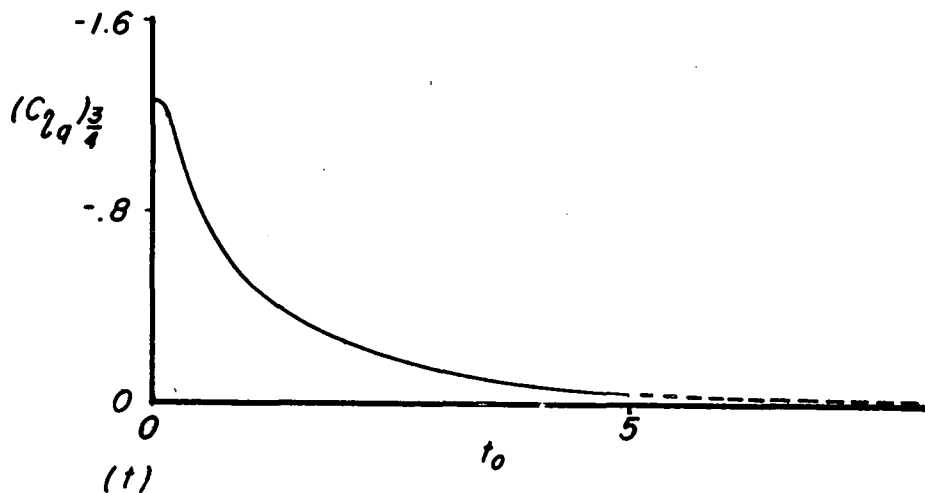


(s)

apparent that the center of pressure is very close to the quarter-chord point for values of $t_0 > 5$. Hence, at $M_0 = 0.8$ the significant effect of compressibility on the location of the center of pressure is contained in the interval $0 \leq t_0 \leq 5$. This leads immediately to the further useful conclusion that for values of t_0 greater than 5 the value of the pitching-moment coefficient is given essentially by the equation

$$c_{m\alpha}' = -c_{l\alpha}/4$$

Likewise, it is apparent from the discussion of the incompressible case that the indicial functions for the pitching wing can also be



expressed in a more convenient form by shifting the axis of rotation from the leading edge to the three-quarter-chord point. Using the values of $c_{l\alpha}$, $c_{m\alpha}'$, c_{lq}' , and c_{mq}' presented in sketch (r), the variation of $(c_{lq}')_{3/4}$ and $(c_{mq}')_{3/4}$ may be calculated from the definitions given in equation (29). These curves are presented in sketches (t) and (u) and again it is apparent that at a Mach number equal to 0.8 the compressibility effects are contained in the interval $0 \leq t_0 \leq 5$.

The later stage.— It follows from the preceding discussion that when t_0 is large, the values of the indicial functions $c_{m\alpha}'$, c_{lq}' , and c_{mq}' for compressible flow can also be expressed adequately in terms of $c_{l\alpha}$ by equations similar to equations (30) which were derived for incompressible flow. Thus for $t_0 > 5$, one can write

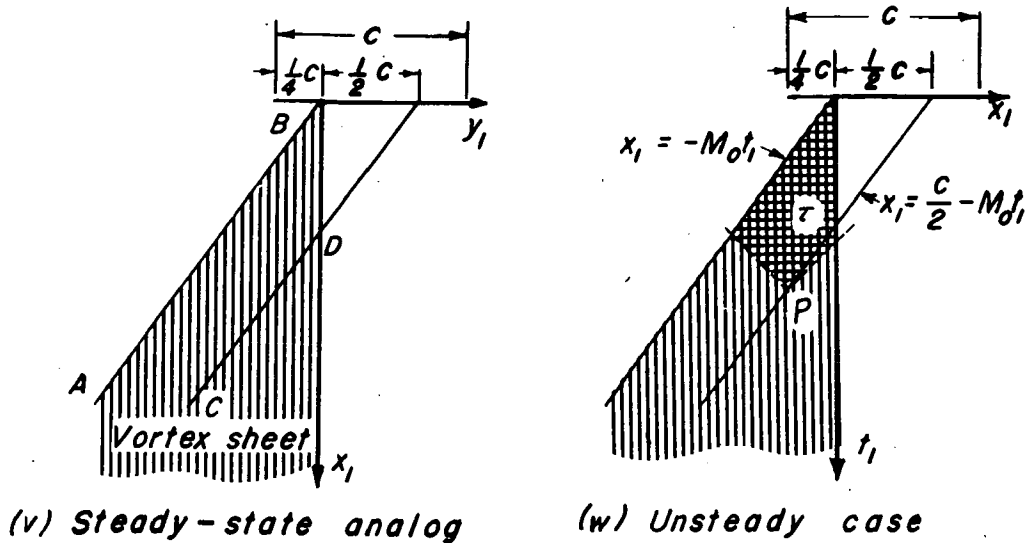
$$\left. \begin{aligned} c_{m\alpha}' &= -c_{l\alpha}'/4 \\ c_{lq}' &= 3c_{l\alpha}'/4 \\ c_{mq}' &= -(3c_{l\alpha}'/16) - (\pi/8\beta) \end{aligned} \right\} \quad (34)$$

The four indicial responses have all been shown to depend only on the value of the function $c_{l\alpha}$ if t_0 is large. It remains, therefore, to determine the asymptotic behavior of $c_{l\alpha}$. This can be accomplished in the following way. Consider the steady-state solution for the lift on a two-dimensional, flat lifting surface traveling at a subsonic Mach number. As was pointed out by Wieghardt (reference 10), if the lift on such a surface is represented by placing at the quarter-chord point a vortex which has the same circulation as that developed by the wing, the angle of attack measured at the three-quarter-chord point will be the same as that of the simulated lifting surface. Extending this concept to include the unsteady effects, an investigation will be made of the variation with time of the vortex strength which will maintain a constant angle of attack at the three-quarter-chord station following an impulsive start at $t_0=0$.

The analogous problem in steady-state theory becomes one of finding the strength of the vortex system, shown in sketch (v), which gives a constant value of w along the line CD.⁵

Each vortex composing this system lies along the line AB, extending from the minus infinity toward the origin, and trails back parallel to

⁵In the vicinity of the origin, of course, this representation gives a poor approximation to the original boundary-value problem; hence, use of the results must be limited to the regions in which t_0 is large.



the x_1 axis to form the trailing vortex sheet. Note that, for convenience, the origin of the axis system has been located at the quarter-chord point. The solution to such a problem in steady-state, lifting-line theory would result from the solution of the integral equation⁶ (for a development using the notation adopted here, see reference 11):

$$w = -\frac{\beta^2}{2\pi} \int_{\tau} dy_1 \int \frac{\Delta\phi(y_1) dx_1}{[(x-x_1)^2 - \beta^2(y-y_1)^2]^{3/2}}$$

where $\Delta\phi$ is not a function of x_1 since the strength of a trailing vortex is, of course, constant. The area of integration τ is the region within the forecone springing from the point x, y .

If the above equation is transformed by means of the analogy to represent the solution of the unsteady problem (see sketch (w)),

⁶The symbols \int and \int are used to indicate that the finite part is to be taken. Thus (see reference 11 or 12),

$$\int_a^b \frac{f(y)dy}{(x-y)^2} \equiv -\frac{\partial}{\partial x} \int_a^b \frac{f(y)dy}{(x-y)} = G(x,b) - G(x,a)$$

where $G(x,y)$ is the indefinite integral of $f(y)/(x-y)^2$. Further,

$$\int_a^x \frac{f(y)dy}{(x-y)^{3/2}} \equiv -2 \frac{\partial}{\partial x} \int_a^x \frac{f(y)}{\sqrt{x-y}} dy$$

β , x , and y are replaced by l , t , and x , respectively; and $\Delta\Phi$, the total jump in potential at a given section, is replaced by the circulation Γ . Hence.

$$w = -\frac{1}{2\pi} \int_{\tau} dx_1 \int \frac{\Gamma(x_1)}{[(t-t_1)^2 - (x-x_1)^2]^{3/2}} dt_1$$

where τ , as indicated in sketch (w), is the area in the forecone from the point P which lies always along the line $x = (1/2)c - M_0 t$. Integration with respect to t_1 reduces the last equation to

$$w = \frac{1}{2\pi} \int \frac{M_0(x-t)}{1+M_0} \frac{\Gamma(x_1) \left[\frac{t+x_1}{M_0} \right] dx_1}{(x-x_1)^2 \sqrt{\left(\frac{t+x_1}{M_0} \right)^2 - (x-x_1)^2}}$$

which, by means of the substitution $x_1/c = x_2/2$ becomes along the line $x = \frac{c}{2} - M_0 t$

$$w = \frac{1}{c\pi\beta} \int_0^{\lambda_0} \frac{(\lambda_0 + \mu_0 - x_2) \Gamma(x_2)}{(\mu_2 - \lambda_0 + x_2)^2 \sqrt{(\lambda_0 - x_2)(\lambda_0 + \mu_1 - x_2)}} dx_2 \quad (35)$$

where $\lambda_0 = 2 M_0 t_0 - \mu_0$, $\mu_0 = M_0/(1+M_0)$, $\mu_1 = 2 M_0/(1-M_0^2)$, $\mu_2 = 1/(1+M_0)$, $t_0 = t/c$, and where, of course, w is a constant equal to $-V_0\alpha$.

A solution for $\Gamma(x_2)$ in the integral equation (35) may be obtained by expanding Γ in a series of the form

$$\Gamma(x_2) = \frac{\pi c \alpha V_0}{\beta} \left[\sqrt{\frac{x_2}{(a_0+x_2)}} + b_1 \sqrt{\frac{x_2}{(a_0+x_2)^3}} + \dots \right] \quad (36)$$

Place equation (36) into (35) and expand in powers of $1/\lambda_0$. There results the expression

$$-\frac{w}{V_0\alpha} = 1 + \frac{c_1}{\lambda_0} + \frac{c_2 \ln(1/\lambda_0)}{\lambda_0^2} + \frac{c_3}{\lambda_0^3} + \dots$$

in which

$$c_1 = b_1 - \frac{a_0}{2} + \frac{1}{\beta^2}$$

Hence, if a_0 and b_1 are chosen so that c_1 is equal to zero, an expression for Γ will be obtained which represents the solution to the integral equation (35) correct to the first order in $1/t_0$ (i.e., $1/\lambda_0$) for large values of t_0 . Further, if equation (36) is expanded in powers of $1/x_2$, there results

$$\Gamma(x_2) = \frac{\pi c \alpha V_0}{\beta} \left[1 + \frac{1}{x_2} \left(b_1 - \frac{a_0}{2} \right) + \dots \right]$$

which becomes, using the condition for c_1 and relating x_2 and t_0 by the equation of the leading edge,

$$\Gamma(t_0) = \frac{\pi c \alpha V_0}{\beta} \left[1 - \frac{1}{2M_0 t_0 \beta^2} + \dots \right] \quad (37)$$

The relation between circulation and lift in incompressible flow has been derived and presented as equation (20). For compressible flow, this expression becomes

$$l = \rho_0 V_0 \Gamma + \rho_0 a_0 \frac{\partial}{\partial t_0} \int_{M_0 t_0}^{1-M_0 t_0} \Delta\Phi(t_0, x_0) dx_0$$

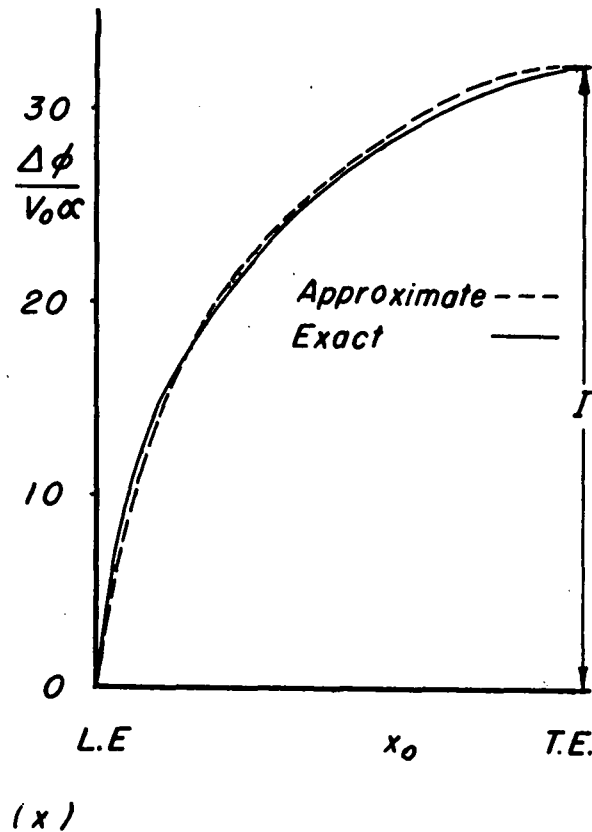
where $x_0 = x/c$. In order to obtain a complete expression for the section lift, it is obviously necessary to know the chordwise variation of $\Delta\Phi$. The asymptotic behavior of l can be calculated, however, by applying the results presented in sketch (q). This result suggests that for large values of t_0 the value of $\Delta\Phi(t_0, x_0)$ used in the equation for section lift can be expressed by the product of $\Delta\Phi(\infty, x_0)$ and $\Gamma(t_0)/\Gamma(\infty)$. In other words, for large values of t_0 the shape of the chordwise distribution of vorticity is the same as the two-dimensional, steady-state value. An indication of the accuracy of such an approximation is shown in sketch (x) where the precise value of $\Delta\Phi(t_0, x_0)$ is compared with the approximation at $t_0=5$.

Since $\Gamma(\infty) = \pi \alpha V_0 c / \beta$, the substitution of

$$\Delta\Phi(t_0, x_0) = \Delta\Phi(\infty, x_0) \Gamma(t_0) / \Gamma(\infty)$$

gives for the lift

$$l = \rho_0 V_0 \Gamma + \frac{3}{4} \rho_0 a_0 \frac{d\Gamma}{dt}$$



Place equation (37) in the above equation and it is evident that, to the first order in $1/t_0$, the section lift is given by $\rho_0 V_0 \Gamma$. Hence, it follows that for large t_0

$$c_{l\alpha} = \frac{2\pi}{\beta} \left(1 - \frac{1}{2M_0 t_0 \beta^2} + \dots \right) \quad (38a)$$

There remains the problem of joining the above result for $c_{l\alpha}$ with the one derived in the preceding section and valid for $0 \leq t_0 \leq 5$. To accomplish this end the equation

$$c_{l\alpha} = \frac{2\pi}{\beta} \left[1 - \frac{1}{h_0 + 2M_0 t_0 \beta^2} - \frac{h_1}{(h_0 + 2M_0 t_0 \beta^2)^2} \right] \quad (38b)$$

was used to express $c_{l\alpha}$ for the range $5 \leq t_0$. Obviously the value of $c_{l\alpha}$ given by equation (38b) has, to the first order in $1/t_0$, the same asymptotic variation as that given by equation (38a) regardless of the values of the constants h_0 and h_1 . These constants can be chosen, therefore, so that both the magnitude and slope of the indicial $c_{l\alpha}$

curve given by equation (38b) are continuous at $t_0=5$ with the exact $c_{l\alpha}$ curve obtained for $0 \leq t_0 \leq 5$ in the previous section.

The curves for $c_{m\alpha}'$, c_{lq}' , and c_{mq}' , as previously discussed, can be calculated from $c_{l\alpha}$ by the use of equations (34). In each of these three cases, the magnitude of h_1 was modified slightly so the resulting curve would be continuous at $t_0=5$ with the exact results presented in the preceding section. The final expressions are

$$\left. \begin{aligned} c_{l\alpha}' &= \frac{2\pi}{\beta} \left[1 - \frac{1.736}{17.06 + t_0} - \frac{131.2}{(17.06 + t_0)^2} \right] \\ c_{m\alpha}' &= \frac{-\pi}{2\beta} \left[1 - \frac{1.736}{17.06 + t_0} - \frac{121.8}{(17.06 + t_0)^2} \right] \\ c_{lq}' &= \frac{3\pi}{2\beta} \left[1 - \frac{1.736}{17.06 + t_0} - \frac{134.3}{(17.06 + t_0)^2} \right] \\ c_{mq}' &= \frac{-\pi}{2\beta} \left[1 - \frac{1.302}{17.06 + t_0} - \frac{90.53}{(17.06 + t_0)^2} \right] \end{aligned} \right\} (39)$$

The final indicial section lift and pitching-moment curves are shown in figure 1 plotted against the parameter V_{ot}'/c , the number of chord lengths traveled ($V_{ot}'/c = M_0 t_0$). Tabular results of the indicial curves are also presented in table I.

Sonic Case, $M_0 = 1.0$

The general results, obtained in the preceding section and presented in appendix A, for the indicial loading over the sinking and pitching wing may be extended to the sonic case. Furthermore, the two intervals for which analytic results in a closed form were presented in appendix A now cover the complete time range since $0 \leq t_0 \leq 1/(1+M_0)$ becomes $0 \leq t_0 \leq 0.5$ and $1/(1+M_0) \leq t_0 \leq 1/(1-M_0)$ becomes $0.5 \leq t_0 \leq \infty$. Hence, by an appropriate limiting process equations (A8), (A9), (A10), and (A11) become for $0 \leq t_0 \leq 0.5$

$$\left. \begin{aligned} c_{l\alpha} &= 4 \\ c_{m\alpha}' &= -2 + t_0^2 \\ c_{lq}' &= 2 + t_0^2 \\ c_{mq}' &= -(4/3) - (2/3)t_0^3 \end{aligned} \right\} (40a)$$

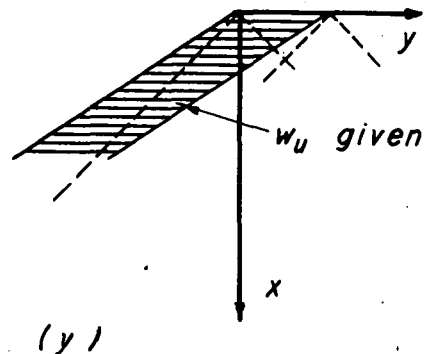
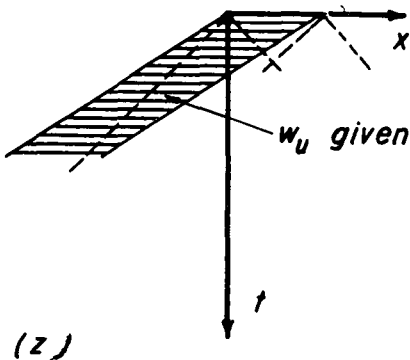
and for $0.5 \leq t_0 \leq \infty$

$$\left. \begin{aligned} c_{l_\alpha} &= (4/\pi) \left(2\sqrt{2t_0-1} + \text{arc. cos } \frac{t_0-1}{t_0} \right) \\ c_{m_\alpha}' &= -(2/\pi) \left[\frac{3+t_0}{2} \sqrt{2t_0-1} + \left(1 - \frac{t_0^2}{2} \right) \text{arc. cos } \frac{t_0-1}{t_0} \right] \\ c_{l_q}' &= (2/\pi) \left[\frac{5t_0}{2} \sqrt{2t_0-1} + \left(1 + \frac{t_0^2}{2} \right) \text{arc. cos } \frac{t_0-1}{t_0} \right] \\ c_{m_q}' &= (4/3\pi) \left[\frac{14-t_0-3t_0^2}{6} \sqrt{2t_0-1} + \left(1 + \frac{t_0^3}{2} \right) \text{arc. cos } \frac{t_0-1}{t_0} \right] \end{aligned} \right\} (40b)$$

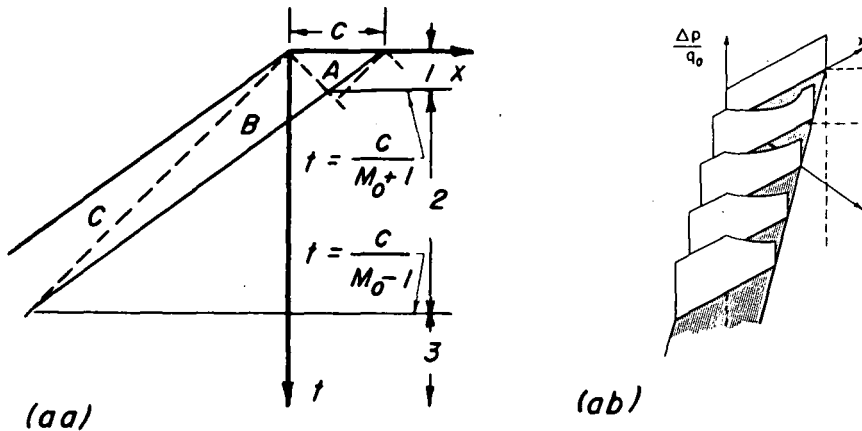
Since the magnitude of the functions in equation (40b) grows indefinitely with increasing time, the assumptions of linear theory are eventually violated. However, for moderate values of t_0 , these functions have the same order of magnitude as similar indicial curves for Mach numbers other than 1. These effects are illustrated in figure 1.

Supersonic Case, $M_0 = 1.2$ and 2

The method of obtaining solutions for the indicial functions at supersonic Mach numbers parallels the development presented for $M_0 = 0.8$. The steady-state analog to the supersonic unsteady wing problem is a constant-chord wing tip with a supersonic trailing edge. See sketches (y) and (z). It is well known that the problem of finding the loading over wing plan forms with all supersonic edges is one of the simplest in three-dimensional, lifting-surface theory. In fact, since the upper and lower surfaces are noninteracting, the solution is determined by integrating sources within the Mach forecone. The analysis for c_{l_α} has already been carried out in reference 5.



The analysis used to calculate the loading in terms of $x_0=x/c$ and $t_0=t/c$ over the three regions shown in sketch (aa) is outlined in appendix B. An example of the manner in which the loading varies with time over a sinking wing traveling at a Mach number equal to 1.2 is given in sketch (ab) and, in more detail, together with the loading over a pitching wing, in figure 3.



The expressions for the indicial lift and pitching-moment coefficients are given analytically in appendix B, and plotted in figure 1. It can be shown that the results given in appendix B reduce to the expressions given by equations (40) when M_0 is allowed to approach one, so that there is no discontinuity in the theory in passing through the sonic range.

CONCLUDING REMARKS

The use of the analogy between the basic flow equations in steady-state, lifting-surface theory and in unsteady-state, airfoil theory has resulted in a method of calculating two-dimensional indicial functions throughout the subsonic and supersonic flight range. The results are, of course, subject to the restrictions of linearized, compressible-flow theory and, for example, the calculated responses given in figure 1 for sonic speeds must be considered as being outside the realm of validity within a few chord lengths of travel. In application to high-frequency oscillations, however, the initial portions of the indicial curves dominate the response characteristics of the airfoil and calculations near M_0 equal to one need not be invalid.

In the supersonic range, the expressions in appendix B are calculated for arbitrary M_0 . It is apparent that no fixed Mach number effect can be used in transient responses except at high values of flight Mach number. In the subsonic range, however, the expressions apply only for the period of time $0 \leq t_0 \leq 1/(1-M_0)$. For values of $t_0 \geq 1/(1-M_0)$,

the method outlined in the report appears to be satisfactory for Mach numbers equal to or greater than 0.8. Preliminary calculations made at Mach numbers less than 0.8 indicate that it is necessary to extend the exact solutions past $t_0 = 1/(1-M_0)$. This extension is feasible if the cancellation techniques outlined in reference 13 are employed and the more difficult integrals are expanded into series form.

Ames Aeronautical Laboratory,
National Advisory Committee for Aeronautics,
Moffett Field, Calif., April 12, 1951.

APPENDIX A

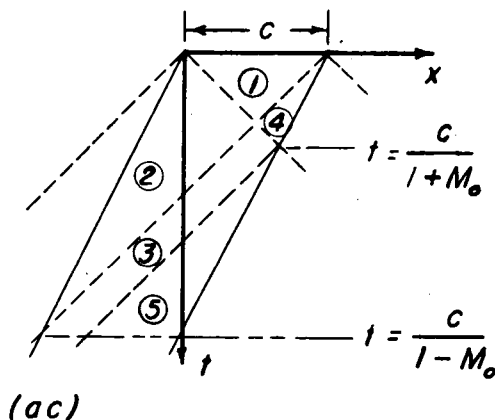
DETERMINATION OF SUBSONIC, INDICIAL, SECTION LIFT AND

PITCHING-MOMENT CURVES

THE LOAD DISTRIBUTION

The following results for the indicial load distribution on sinking or pitching wings can be obtained in two ways. One of these methods will be outlined in the subsequent paragraphs. The other is outlined in references 13 and 14 and is referred to as the lift-cancellation technique. The latter method has been used to check the load distributions originally obtained by the former so that an independent check of these results has been carried out.

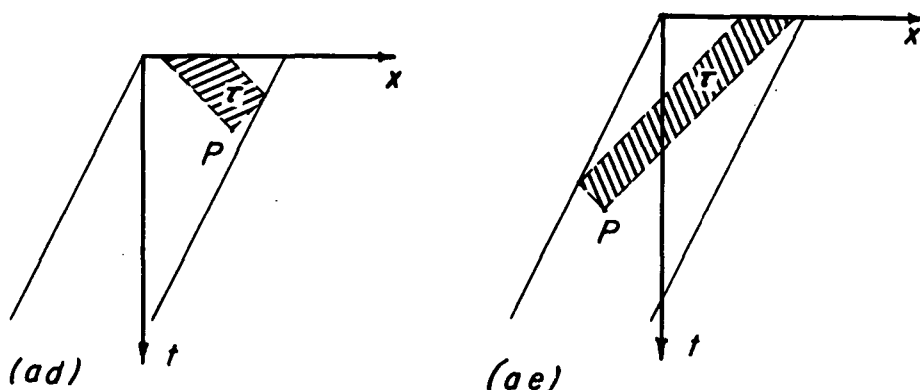
It was shown that the lifting-surface analog to the solution for load distribution over an unsteady, two-dimensional wing traveling at a constant subsonic speed involved the calculation of load distribution over a swept-forward wing tip with subsonic edges. Sketch (ac) indicates the geometry associated with the boundary conditions, and the solutions are calculated for the various regions shown.



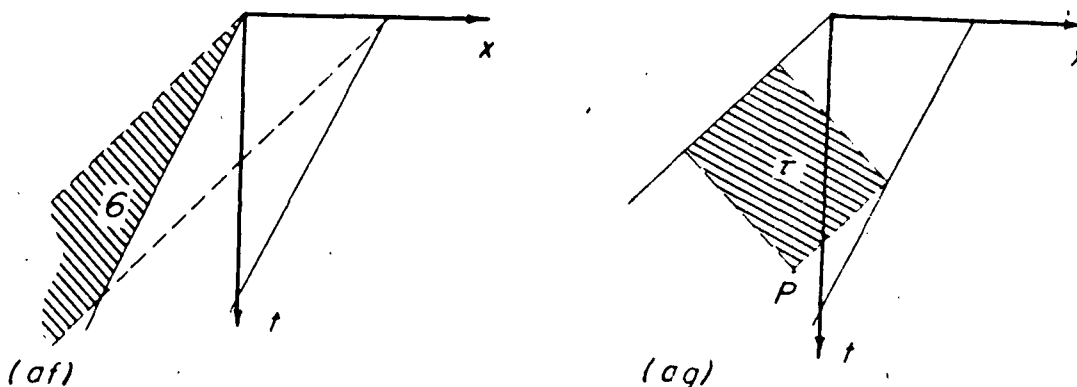
In the notation of the unsteady problem the expression for the velocity potential can be written

$$\phi = -\frac{1}{\pi} \iint_{\tau} \frac{(w_u) dt_1 dx_1}{\sqrt{(t-t_1)^2 - (x-x_1)^2}} \quad (A1)$$

where τ is the area on the wing plan form included in the Mach forecone from the point (t,x) . Equation (A1) is applicable only for cases in which w_u is known at all points within the forecone, as is the case when the edge of the wing within the forecone is everywhere supersonic (i.e., region 1 in sketch (ac)). However, Evvard (reference 8) has extended the solution provided by equation (A1) to include cases such as shown in sketches (ad) and (ae) in which the forecone intersects a subsonic edge and includes a region of unknown upwash. As was pointed out in reference 8, equation (A1) applies in these instances if the area of integration τ is limited to the shaded regions shown in the sketches. It is apparent, therefore, that the potential (and thus the loading) over a sinking or pitching wing can readily be determined for regions 1, 2, and 4 in sketch (ac).



Points in regions 3 and 5 have forecones which intersect two subsonic edges, and the method just discussed can no longer be directly applied. In reference 8, however, a method was given of evaluating the upwash in the region between the Mach cone from the apex and the leading edge (region 6 in sketch (af)). Thus, the plan form has become, effectively, one such as shown in sketch (ag) in which only one edge is subsonic. This reduces the problem of finding the potential in these regions to the same problem as was involved in region 4. The analysis used in finding the loading over the various regions will now be considered.



First, introduce a new coordinate system in which the lines $x = -t$ and $x = t$ are taken as the r and s axes, respectively, (see sketch (ah)). (This amounts to a rotation of the original axial system through an angle of 45° .) The transformations relating the r, s to the x, y system are

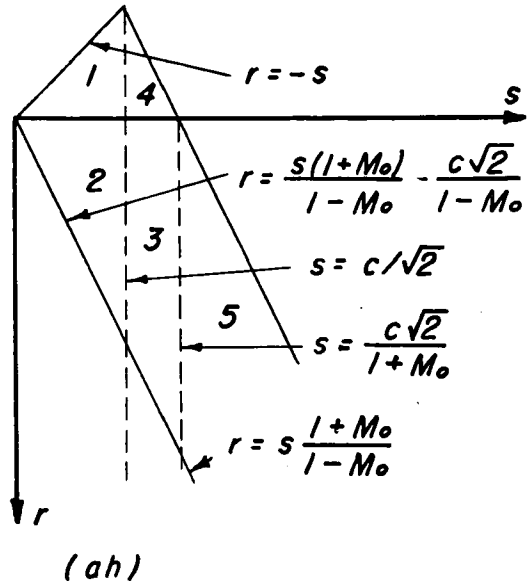
$$r = \frac{1}{\sqrt{2}} (t-x) \quad t = \frac{1}{\sqrt{2}} (r+s)$$

$$s = \frac{1}{\sqrt{2}} (t+x) \quad x = \frac{1}{\sqrt{2}} (s-r)$$

In the new coordinate system equation (A1) is written

$$\phi = -\frac{1}{\pi\sqrt{2}} \int \int_T \frac{(w_u) dr_1 ds_1}{\sqrt{(r-r_1)(s-s_1)}} \quad (A2)$$

The vertical induced velocity w_u over the wing plan form is given in equations (5) and (6) for the sinking wing and pitching wing, respectively. The method developed in reference 8 was used to obtain the value of w_u over the area between the lines $s=0$ and $r=s(1+M_0)/(1-M_0)$ (region 6 in sketch (af)). The results for the sinking and pitching wing are, respectively,



$$w_u = \frac{2V_0\alpha}{\pi} \left[\sqrt{\frac{2s}{(r-s)-M_0(r+s)}} - \arctan \sqrt{\frac{2s}{(r-s)-M_0(r+s)}} \right]$$

$$w_u = \frac{2\dot{\theta}}{\pi} \frac{1}{\sqrt{2}} \left\{ \left[(r-s)-M_0(r+s) - \frac{2s}{3} \right] \sqrt{\frac{2s}{(r-s)-M_0(r+s)}} - \left[(r-s)-M_0(r+s) \right] \arctan \sqrt{\frac{2s}{(r-s)-M_0(r+s)}} \right\} \quad (A3)$$

In terms of the r,s coordinate system, the expression for the loading can be written

$$\frac{\Delta p}{q_0} = \frac{4}{V_0 M_0} \frac{1}{\sqrt{2}} \left(\frac{\partial}{\partial r} + \frac{\partial}{\partial s} \right) \phi \quad (A4)$$

If the subsonic trailing edge is not included in the forecone from the point at which the loading is being determined, the expression for ϕ may be substituted directly into equation (A4). However, if the trailing edge is included in the forecone, and if the Kutta condition is to apply along such an edge, it can be shown that the equation for the loading coefficient assumes the form

$$\frac{\Delta p}{q_0} = -\frac{2}{\pi V_0 M_0} \int_T \frac{dr_1}{\sqrt{r-r_1}} \left(\frac{\partial}{\partial r_1} + \frac{\partial}{\partial s} \right) \int \frac{(w_u) ds_1}{\sqrt{s-s_1}} \quad (A5)$$

Sinking Wing

The preceding method can be applied to the sinking wing to obtain the following integral relationship for the loading over the various regions. The subscripts on $\left(\frac{\Delta p}{q_0} \right)$ indicate the region for which the particular equation applies.

$$\frac{1}{\alpha} \left(\frac{\Delta p}{q_0} \right)_1 = \frac{2}{\pi M_0} \left(\frac{\partial}{\partial r} + \frac{\partial}{\partial s} \right) \int_{-s}^r \frac{dr_1}{\sqrt{r-r_1}} \int_{-r_1}^s \frac{ds}{\sqrt{s-s_1}}$$

$$\frac{1}{\alpha} \left(\frac{\Delta p}{q_0} \right)_2 = \frac{2}{\pi M_0} \left(\frac{\partial}{\partial r} + \frac{\partial}{\partial s} \right) \int_{\frac{r(1-M_0)}{(1+M_0)}}^s \frac{ds_1}{\sqrt{s-s_1}} \int_{-s_1}^r \frac{dr_1}{\sqrt{r-r_1}}$$

$$\frac{1}{\alpha} \left(\frac{\Delta p}{q_0} \right)_3 = \frac{2}{\pi M_0} \left\{ \int_0^r \frac{dr_1}{\sqrt{r-r_1}} \left(\frac{\partial}{\partial r_1} + \frac{\partial}{\partial s} \right) \int_{\frac{r_1(1-M_0)}{(1+M_0)}}^s \frac{ds_1}{\sqrt{s-s_1}} + \right.$$

$$\int_0^r \frac{dr_1}{\sqrt{r-r_1}} \left(\frac{\partial}{\partial r_1} + \frac{\partial}{\partial s} \right) \int_0^{\frac{r_1(1-M_0)}{(1+M_0)}} \frac{ds_1}{\sqrt{s-s_1}} - \left. \frac{2}{\pi} ds_1 \left[\frac{\sqrt{\frac{2s_1}{(r_1-s_1)-M_0(r_1+s_1)}} - \arctan \sqrt{\frac{2s_1}{(r_1-s_1)-M_0(r_1+s_1)}}}{\sqrt{s-s_1}} \right] + \right.$$

$$\left. \int_{r_d}^0 \frac{dr_1}{\sqrt{r-r_1}} \left(\frac{\partial}{\partial r_1} + \frac{\partial}{\partial s} \right) \int_{-r_1}^s \frac{ds_1}{\sqrt{s-s_1}} \right\}$$

$$\frac{1}{\alpha} \left(\frac{\Delta p}{q_0} \right)_4 = \frac{2}{\pi M_0} \int_{r_d}^r \frac{dr_1}{\sqrt{r-r_1}} \left(\frac{\partial}{\partial r_1} + \frac{\partial}{\partial s} \right) \int_{-r_1}^s \frac{ds}{\sqrt{s-s_1}}$$

$$\frac{1}{\alpha} \left(\frac{\Delta p}{q_0} \right)_5 = \frac{2}{\pi M_0} \left\{ \int_{r_d}^r \frac{dr_1}{\sqrt{r-r_1}} \left(\frac{\partial}{\partial r_1} + \frac{\partial}{\partial s} \right) \int_{\frac{r_1(1-M_0)}{(1+M_0)}}^s \frac{ds_1}{\sqrt{s-s_1}} + \int_{r_d}^r \frac{dr_1}{\sqrt{r-r_1}} \left(\frac{\partial}{\partial r_1} + \frac{\partial}{\partial s} \right) \int_0^{\frac{r_1(1-M_0)}{(1+M_0)}} - \frac{2}{\pi} ds_1 \right. \\ \left. \left[\frac{\sqrt{\frac{2s_1}{(r_1-s_1)-M_0(r_1+s_1)}} - \arctan \sqrt{\frac{2s_1}{(r_1-s_1)-M_0(r_1+s_1)}}}{\sqrt{s-s_1}} \right] \right\}$$

where

$$r_d = \frac{s(1+M_0) - c\sqrt{2}}{1-M_0}$$

Most of these integrals can be readily evaluated to give

$$\frac{1}{\alpha} \left(\frac{\Delta p}{q_0} \right)_1 = \frac{4}{M_0} \tag{A6a}$$

$$\frac{1}{\alpha} \left(\frac{\Delta p}{q_0} \right)_2 = \frac{8}{\pi M_0} \left(\frac{M_0}{1+M_0} \sqrt{\frac{t_0-x_0}{M_0 t_0+x_0}} + \arctan \sqrt{\frac{M_0 t_0+x_0}{t_0-x_0}} \right) \tag{A6b}$$

$$\frac{1}{\alpha} \left(\frac{\Delta p}{q_0} \right)_3 = \frac{8}{\pi(1+M_0)} \sqrt{\frac{t_0-x_0}{M_0 t_0+x_0}} + \frac{4}{\pi M_0} \left[\arcsin \frac{2x_0-t_0(1-M_0)}{(1+M_0)t_0} + \arcsin \frac{2(1-x_0)-t_0(1+M_0)}{t_0(1-M_0)} \right] \tag{A6c}$$

$$\frac{1}{\alpha} \left(\frac{\Delta p}{q_0} \right)_4 = \frac{8}{\pi M_0} \arcsin \sqrt{\frac{x_0-1+M_0 t_0}{t_0(M_0-1)}} \tag{A6d}$$

$$\frac{1}{\alpha} \left(\frac{\Delta p}{q_0} \right)_5 = \frac{16}{\pi^2(1+M_0)} \sqrt{\frac{t_0-x_0}{M_0 t_0+x_0}} \left[\frac{\pi}{2} - \text{EF}(\psi, k') - \text{KE}(\psi, k') + \text{KF}(\psi, k') \right] -$$

$$\frac{2}{\pi M_0} \arcsin \frac{x}{t} + \frac{4}{\pi M_0} \arcsin \frac{2x-t(1-M_0)}{(1+M_0)t} +$$

$$\frac{32K}{\pi^2(1+M_0)} \sqrt{\frac{1-x_0-M_0 t_0}{(1-M_0^2)(x_0+t_0)}} - \frac{2}{\pi M_0} \arcsin \frac{2-t_0(1+M_0)}{t_0(1+M_0)} + G_1$$

(A6e)

where

$$k' = \sqrt{1-k^2}$$

$$k = \sqrt{1 - \frac{2}{(t_0+x_0)(1+M_0)}}$$

$$\psi = \arcsin \sqrt{x_0 + M_0 t_0}$$

$$G_1 = \frac{4}{\pi^2 M_0} \int_0^{s - \frac{c\sqrt{2}}{1+M_0}} \left\{ \left[\frac{ds_1}{\sqrt{(s-s_1)(r+s_1)}} \right] \right.$$

$$\left. \arcsin \frac{(r+s_1)(1-M_0)[(s-s_1)(1+M_0) - c\sqrt{2}] + 2s_1[s(1+M_0) - c\sqrt{2} - r(1-M_0)]}{[s(1+M_0) - c\sqrt{2} + s_1(1-M_0)][r(1-M_0) - s_1(1+M_0)]} \right\}$$

Pitching Wing

A similar analysis of the pitching wing yields the following results for the loading coefficient:

$$\frac{1}{\alpha} \left(\frac{\Delta p}{q_0} \right)_1 = \frac{4}{M_0} \left(M_0 t_0 + x_0 \right) \quad (A7a)$$

$$\frac{1}{q} \left(\frac{\Delta p}{q_0} \right)_2 = \frac{8}{3\pi M_0} \left[\frac{M_0(1-M_0)}{(1+M_0)^2} \frac{(t_0-x_0)^{3/2}}{\sqrt{M_0 t_0+x_0}} + 3\sqrt{(t_0-x_0)(M_0 t_0+x_0)} + 3(M_0 t_0+x_0) \arctan \sqrt{\frac{M_0 t_0+x_0}{t_0-x_0}} \right] \quad (A7b)$$

$$\frac{1}{q} \left(\frac{\Delta p}{q_0} \right)_3 = \frac{8}{\pi M_0} \left\{ \sqrt{(t_0-x_0)(M_0 t_0+x_0)} + \frac{1}{3} \frac{M_0(1-M_0)}{(1+M_0)^2} \sqrt{\frac{(t_0-x_0)^3}{M_0 t_0+x_0}} - \sqrt{[1-(M_0 t_0+x_0)][(t_0+x_0)-1]} + (M_0 t_0+x_0) \left[\arctan \sqrt{\frac{1-(M_0 t_0+x_0)}{(t_0+x_0)-1}} - \arctan \sqrt{\frac{t_0-x_0}{M_0 t_0+x_0}} \right] \right\} \quad (A7c)$$

$$\frac{1}{q} \left(\frac{\Delta p}{q_0} \right)_4 = \frac{8}{\pi M_0} \left\{ (M_0 t_0+x_0) \arctan \sqrt{\frac{1-(M_0 t_0+x_0)}{t_0+x_0-1}} - \sqrt{(t_0+x_0-1)[1-(M_0 t_0+x_0)]} \right\} \quad (A7d)$$

$$\frac{1}{q} \left(\frac{\Delta p}{q_0} \right)_5 = \frac{8}{\pi M_0} \left\{ \frac{M_0}{\sqrt{1-M_0^2}} \left[\sqrt{1-(M_0 t_0+x_0)} + (M_0 t_0+x_0) \tanh^{-1} \sqrt{1-(M_0 t_0+x_0)} \right] - \frac{\sqrt{(t_0-x_0)(t_0+x_0)}}{2} + \sqrt{(t_0-x_0)(M_0 t_0+x_0)} + \frac{M_0(1-M_0)}{3(1+M_0)^2} \sqrt{\frac{(t_0-x_0)^3}{M_0 t_0+x_0}} - (M_0 t_0+x_0) \left[\arctan \sqrt{\frac{t_0+x_0}{t_0-x_0}} - \arctan \sqrt{\frac{M_0 t_0+x_0}{t_0-x_0}} + \right. \right. \left. \left. \right] \right\}$$

$$\left. \frac{M_0}{\sqrt{1-M_0^2}} \tanh^{-1} \sqrt{\frac{(t_0-x_0)(1-M_0)}{(t_0+x_0)(1+M_0)}} \right] \} + \frac{1}{c} G_2 \quad (A7e)$$

where

$$G_2 = -\frac{4}{\pi^2 M_0} \int_0^{\frac{r_d(1-M_0)}{1+M_0}} \frac{ds_1}{\sqrt{s-s_1}} \left\{ \left(-2M_0 \sqrt{r+s_1} - \frac{2s_1}{\sqrt{r+s_1}} \right) \right. \\ \left[\text{arc tan } \frac{-4s_1(r+s_1) + (r_d+s_1)[r(1-M_0) + s_1(1+M_0) + 2s_1(1-M_0)]}{2\sqrt{2s_1(r+s_1)}(r-r_d)[r_d(1-M_0)-s_1(1+M_0)]} + \frac{\pi}{2} \right] - \\ 4M_0 \sqrt{r-r_d} \text{arc tan } \sqrt{\frac{2s_1}{r_d(1-M_0)-s_1(1+M_0)}} + \frac{2M_0\pi}{\sqrt{1-M_0}} \sqrt{r(1-M_0)-s_1(1+M_0)} + \\ \left. \frac{2}{3} \frac{M_0}{1+M_0} \left[\frac{(2s_1)^{3/2}}{s-s_1} + 6\sqrt{2s_1} \right] \frac{1}{\sqrt{1-M_0}} \text{arc tan } \sqrt{\frac{r_d(1-M_0)-s_1(1+M_0)}{(1-M_0)(r-r_d)}} \right\}$$

LIFT AND PITCHING-MOMENT COEFFICIENTS

The lift and pitching-moment coefficients may be obtained by suitable integrations of equations (A6) and (A7) and are given in the time intervals indicated in sketch (aa) by the following expressions:

Sinking wing

$$0 \leq t_0 \leq \frac{1}{1+M_0}$$

$$c_{l\alpha} = \frac{4}{M_0} \left[1-t_0(1-M_0) \right] \quad (A8a)$$

$$c_{m\alpha} = -\frac{4}{M_0} \left[\frac{1}{2} - \frac{t_0}{2} (1-M_0) + \frac{t_0^2 M_0}{4} (M_0-2) \right] \quad (A9a)$$

$$\frac{1}{1+M_0} \leq t_0 \leq \frac{1}{1-M_0}$$

$$\begin{aligned}
 c_{l\alpha} = \frac{4}{\pi M_0} & \left\{ \frac{4-3t_0(1-M_0^2)}{1+M_0} \arctan \sqrt{\frac{2-t_0(1-M_0^2)}{2t_0(1+M_0)-2}} + \right. \\
 & \pi \left(t_0 - \frac{2}{1+M_0} \right) + \frac{1+3M_0}{(1+M_0)^2} \sqrt{[2t_0(1+M_0)-2][2-t_0(1-M_0^2)]} + \\
 & \frac{4-2t_0(1+M_0)}{1+M_0} \arcsin \sqrt{\frac{t_0(1+M_0)-1}{t_0(1+M_0)}} - \\
 & \left. \frac{1-M_0}{1+M_0} \sqrt{t_0(1+M_0)-1} + [2-t_0(1+M_0)] \arctan \sqrt{\frac{1}{t_0(1+M_0)-1}} \right\} + \\
 & \int_{\frac{2}{1+M_0} - t_0}^{1-M_0 t_0} \left(\frac{\Delta p}{q_0} \right)_5 dx_0 \tag{A8b}
 \end{aligned}$$

where $\left(\frac{\Delta p}{q_0} \right)_5$ is given by equation (A6e)

$$\begin{aligned}
 c_{m\alpha}' = -\frac{8}{\pi M_0} & \left\{ \left[\frac{t_0^2(5-18M_0+9M_0^2)}{16} + \frac{2t_0(M_0-1)}{1+M_0} + \frac{2}{(1+M_0)^2} \right] \right. \\
 & \arctan \sqrt{\frac{2-t_0(1-M_0^2)}{2[t_0(1+M_0)-1]}} + \left[\frac{-5t_0^2(1-M_0)^2}{16} + \frac{t_0(M_0^2-4M_0+3)}{2(1+M_0)} + \frac{M_0^2+2M_0-3}{2(1+M_0)^2} \right] \\
 & \arctan \frac{1}{\sqrt{t_0(1+M_0)-1}} + \frac{\sqrt{2[2-t_0(1-M_0^2)][t_0(1+M_0)-1]}}{1+M_0} \left[\frac{t_0(1-6M_0+9M_0^2)}{16(1+M_0)} + \right. \\
 & \left. \frac{1+5M_0}{4(1+M_0)^2} \right] + \frac{1-M_0}{1+M_0} \sqrt{t_0(1+M_0)-1} \left[\frac{5t_0(1-M_0)}{16} - \frac{5+3M_0}{8(1+M_0)} \right] \left. \right\} - \\
 & \int_{\frac{2}{1+M_0} - t_0}^{1-M_0 t_0} (x_0+M_0 t_0) \left(\frac{\Delta p}{q_0} \right)_5 dx_0 \tag{A9b}
 \end{aligned}$$

Pitching wing

$$0 \leq t_0 \leq \frac{1}{1+M_0}$$

$$c_{lq}' = \frac{2}{M_0} \left[t_0^2 \left(M_0 - \frac{M_0^2}{2} \right) + t_0(M_0-1) + 1 \right] \tag{A10a}$$

$$c_{mq}' = -\frac{4}{3M_0} \left\{ t_0^3 \left[\frac{1}{8} (1-M_0)^3 + \frac{1}{2} M_0 \right] + \frac{3}{8} t_0^2 (1-M_0)^2 - \frac{3}{2} t_0 (1-M_0) + 1 \right\} \quad (A11a)$$

$$\frac{1}{1+M_0} \leq t_0 \leq \frac{1}{1-M_0}$$

$$c_{lq}' = \frac{8}{\pi M_0} \left\{ \sqrt{t_0+t_0 M_0-1} \left[\frac{t_0(-5M_0^2+2M_0-3)}{12(1+M_0)} + \frac{5M_0^2+7M_0+3}{3(1+M_0)^2} \right] - \right. \\ \left. \sqrt{t_0^2-(1-M_0 t_0)^2} \left(\frac{3}{8} - \frac{M_0 t_0}{8} \right) + \left[t_0^2 \frac{(-M_0^2+2M_0+1)}{4} - t_0 \frac{(1-M_0)}{2} + 1 \right] \right. \\ \left. \arcsin \sqrt{\frac{1}{t_0+t_0 M_0-1}} - \left(\frac{t_0^2}{4} + \frac{1}{2} \right) \left[\arcsin \sqrt{\frac{t_0+1-t_0 M_0}{t_0+t_0 M_0-1}} \right] - \right. \\ \left. \frac{1}{2} \frac{M_0}{\sqrt{1-M_0^2}} \tanh^{-1} \sqrt{\frac{(1-M_0)(t_0+t_0 M_0-1)}{(1+M_0)(t_0+1-t_0 M_0)}} \right\} + \int_{-t_0+\frac{2}{1+M_0}}^{1-M_0 t_0} \frac{G_2}{c} dx_0 \quad (A10b)$$

where G_2 is defined under equation (A7e).

$$c_{mq}' = -\frac{8}{\pi M_0} \left\{ -\frac{1}{3} \frac{M_0}{\sqrt{1-M_0^2}} \tanh^{-1} \sqrt{\frac{(1-M_0)(t_0(1+M_0)-1)}{(1+M_0)(t_0(1-M_0)+1)}} - \right. \\ \left[-\frac{t_0^3}{24} (M_0+1)(-M_0^2+4M_0+1) - \frac{t_0^2}{8} (1-M_0)^2 + \frac{t_0}{2} (1-M_0) - \frac{2}{3} \right] \\ \arcsin \sqrt{\frac{1}{t_0(1+M_0)-1}} - \left(\frac{M_0 t_0^3}{6} + \frac{1}{3} \right) \arcsin \sqrt{\frac{t_0(1-M_0)+1}{t_0(1+M_0)-1}} + \\ \sqrt{t_0(1+M_0)-1} \left\{ \frac{-t_0^2[(1-M_0)^3+8M_0]}{24(1+M_0)} + \frac{t_0(9M_0^2-6M_0-11)}{72(1+M_0)} + \right. \\ \left. \frac{39M_0^2+54M_0+19}{36(1+M_0)^2} \right\} + \sqrt{t_0^2-(1-M_0 t_0)^2} \left[\frac{t_0^2(2+M_0^2) + t_0 M_0 - 8}{36} \right] \right\} + \\ \int_{-t_0+\frac{2}{1+M_0}}^{1-M_0 t_0} (x_0+M_0 t_0) \left(\frac{G_2}{c} \right) dx_0 \quad (A11b)$$

APPENDIX B

DETERMINATION OF SUPERSONIC, INDICIAL, SECTION LIFT AND
 PITCHING MOMENT CURVES
 THE LOAD DISTRIBUTION

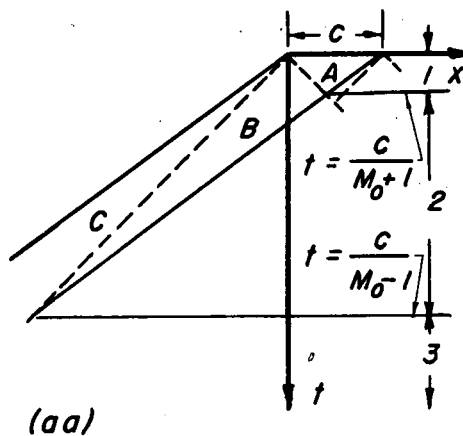
In the case of the unsteady supersonic wing the expression for the velocity potential may be readily obtained by placing the values of w_u given by equations (5) and (6) in the equation

$$\phi = -\frac{1}{\pi} \iint_{\tau} \frac{w_u dx_1}{\sqrt{(t-t_1)^2 - (x-x_1)^2}} \tag{B1}$$

where τ is the area on the plan form included in the Mach forecone. The loading may then be calculated from the relationship given in equation (4).

Sinking Wing

The load distribution over the regions A, B, and C shown in sketch (aa) are given by the following expressions:



$$\frac{1}{\alpha} \left(\frac{\Delta p}{q_0} \right)_A = \frac{4}{M_0} \tag{B2a}$$

$$\frac{1}{\alpha} \left(\frac{\Delta p}{q_0} \right)_B = \frac{4}{\sqrt{M_0^2 - 1}} \left[\frac{1}{\pi} \arccos \frac{M_0 x_0 + t_0}{x + M_0 t_0} + \frac{\sqrt{M_0^2 - 1}}{\pi M_0} \arccos \left(-\frac{x_0}{t_0} \right) \right] \quad (B2b)$$

$$\frac{1}{\alpha} \left(\frac{\Delta p}{q_0} \right)_C = \frac{4}{\sqrt{M_0^2 - 1}} \quad (B2c)$$

Pitching Wing

For the case of the pitching wing the values of $\frac{1}{q} \left(\frac{\Delta p}{q_0} \right)$ in regions A, B, and C are, respectively,

$$\frac{1}{q} \left(\frac{\Delta p}{q_0} \right)_A = \frac{4}{M_0} (x_0 + M_0 t_0) \quad (B3a)$$

$$\frac{1}{q} \left(\frac{\Delta p}{q_0} \right)_B = \frac{4}{\pi} \left[\frac{x_0 + M_0 t_0}{\sqrt{M_0^2 - 1}} \arccos \frac{M_0 x_0 + t_0}{x_0 + M_0 t_0} + \frac{x_0 + M_0 t_0}{M_0} \arccos \left(-\frac{x_0}{t_0} \right) + \sqrt{t_0^2 - x_0^2} \right] \quad (B3b)$$

$$\frac{1}{q} \left(\frac{\Delta p}{q_0} \right)_C = \frac{4}{\sqrt{M_0^2 - 1}} (x_0 + M_0 t_0) \quad (B3c)$$

LIFT AND PITCHING-MOMENT COEFFICIENTS

The lift and pitching-moment coefficients may be obtained by suitable integrations of equations (B2) and (B3) and are given in the time intervals indicated in sketch (aa) by the following expressions:

Sinking wing

$$0 \leq t_0 \leq \frac{1}{1 + M_0}$$

$$c_{l\alpha} = \frac{4}{M_0} \quad (B4a)$$

$$c_{m\alpha} = -\frac{1}{M_0} (2 - t_0^2) \quad (B5a)$$

$$\frac{1}{1+M_0} \leq t_0 \leq \frac{1}{M_0-1}$$

$$c_{l\alpha} = \frac{4}{\pi} \left[\frac{1}{M_0} \arccos \frac{M_0 t_0 - 1}{t_0} + \frac{1}{\sqrt{M_0^2 - 1}} \arccos (t_0 + M_0 - t_0 M_0^2) + \frac{1}{M_0} \sqrt{t_0^2 - (1 - M_0 t_0)^2} \right] \quad (B4b)$$

$$c_{m\alpha}' = -\frac{2}{\pi} \left[\frac{1}{M_0} \left(1 - \frac{t_0^2}{2} \right) \arccos \frac{M_0 t_0 - 1}{t_0} + \frac{1}{\sqrt{M_0^2 - 1}} \arccos (t_0 + M_0 - t_0 M_0^2) + \frac{1}{M_0} \left(\frac{1 + M_0 t_0}{2} \right) \sqrt{t_0^2 - (1 - M_0 t_0)^2} \right] \quad (B5b)$$

$$\frac{1}{M_0 - 1} \leq t_0 \leq \infty$$

$$c_{l\alpha} = \frac{4}{\sqrt{M_0^2 - 1}} \quad (B4c)$$

$$c_{m\alpha}' = -\frac{2}{\sqrt{M_0^2 - 1}} \quad (B5c)$$

Pitching wing

$$0 \leq t_0 \leq \frac{1}{1+M_0}$$

$$c_{lq}' = \frac{2}{M_0} \left(1 + \frac{t_0^2}{2} \right) \quad (B6a)$$

$$c_{mq}' = -\frac{4}{3M_0} \left(1 + \frac{M_0 t_0^3}{2} \right) \quad (B7a)$$

$$\frac{1}{1+M_0} \leq t_0 \leq \frac{1}{M_0-1}$$

$$c_{lq}' = \frac{2}{\pi} \left[\frac{1}{M_0} \left(1 + \frac{t_0^2}{2} \right) \arccos \frac{M_0 t_0 - 1}{t_0} + \frac{1}{\sqrt{M_0^2 - 1}} \arccos (t_0 + M_0 - t_0 M_0^2) + \frac{(3 - M_0 t_0)}{2M_0} \sqrt{t_0^2 - (1 - M_0 t_0)^2} \right] \quad (B6b)$$

$$c_{mq}' = -\frac{4}{3\pi} \left[\frac{1}{M_0} \left(1 + \frac{M_0 t_0^3}{2} \right) \arccos \frac{M_0 t_0 - 1}{t_0} + \frac{1}{\sqrt{M_0^2 - 1}} \right. \\ \left. \arccos (t_0 + M_0 - t_0 M_0^2) + \frac{(8 - M_0 t_0 - 2t_0^2 - M_0^2 t_0^2)}{6M_0} \sqrt{t_0^2 - (1 - M_0 t_0)^2} \right] \quad (B7b)$$

$$\frac{1}{M_0 - 1} \leq t_0 \leq \infty$$

$$c_{lq}' = \frac{2}{\sqrt{M_0^2 - 1}} \quad (B6c)$$

$$c_{mq}' = -\frac{4}{3\sqrt{M_0^2 - 1}} \quad (B7c)$$

REFERENCES

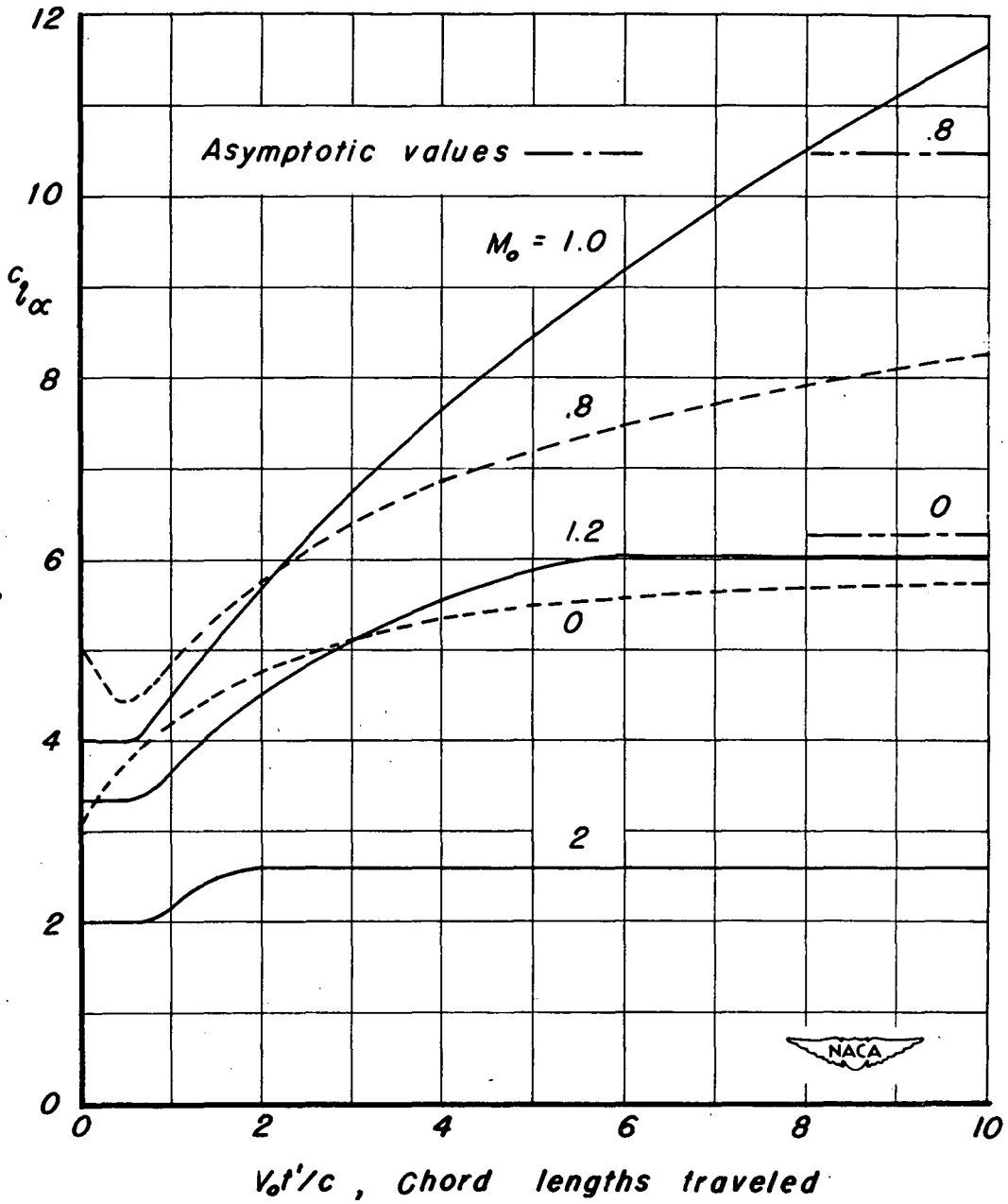
1. Wagner, Herbert: Über die Entstehung des dynamischen Auftriebes von Tragflügeln. z.f.a.M.M., Bd. 5, Heft 1, Feb. 1925, S.17-35.
2. Garrick, I. E.: On Some Reciprocal Relations in the Theory of Non-stationary Flows. NACA Rep. 629, 1938.
3. Theodorsen, Theodore: General Theory of Aerodynamic Instability and the Mechanism of Flutter. NACA Rep. 496, 1935.
4. Garrick, I. E., and Rubinow, S. I.: Flutter and Oscillating Air-Foil Calculations for an Airfoil in a Two-Dimensional Supersonic Flow. NACA Rep. 846, 1946. (Formerly TN 1158)
5. Heaslet, Max. A., and Lomax, Harvard: Two-Dimensional Unsteady Lift Problems in Supersonic Flight. NACA Rep. 945, 1949. (Formerly TN 1621)
6. Jones, Robert T.: Properties of Low-Aspect-Ratio Pointed Wings at Speeds Below and Above the Speed of Sound. NACA Rep. 835, 1946. (Formerly TN 1032)
7. Lomax, Harvard, and Heaslet, Max. A.: Linearized Lifting-Surface Theory for Swept-Back Wings with Slender Plan Forms. NACA TN 1992, 1949.
8. Esvard, John C.: Use of Source Distributions for Evaluating Theoretical Aerodynamics of Thin Finite Wings at Supersonic Speeds. NACA Rep. 951, 1950.
9. Cohen, Doris: Theoretical Loading at Supersonic Speeds of Flat Swept-Back Wings with Interacting Trailing and Leading Edges. NACA TN 1991, 1949.
10. Wieghardt, K.: Chordwise Load Distribution of a Simple Rectangular Wing. NACA TM No. 963, 1940.
11. Lomax, Harvard, Heaslet, Max. A., and Fuller, Franklyn B.: Formulas for Source, Doublet and Vortex Distributions in Supersonic Wing Theory. NACA TN 2252, 1950.
12. Ribner, Herbert S.: Some Conical and Quasi-Conical Flows in Linearized Supersonic-Wing Theory. NACA TN 2147, 1950.
13. Mirels, Harold: Lift-Cancellation Technique in Linearized Supersonic-Wing Theory. NACA TN 2145, 1950.
14. Goodman, Theodore R.: The Lift Distribution on Conical and Non-conical Flow Regions of Thin Finite Wings in a Supersonic Stream. Jour. Aero. Sci., vol. 16, no. 6, June 1949, pp. 365-374.

TABLE I

TABULAR VALUES OF SUBSONIC INDICIAL
LIFT AND PITCHING MOMENT CURVES

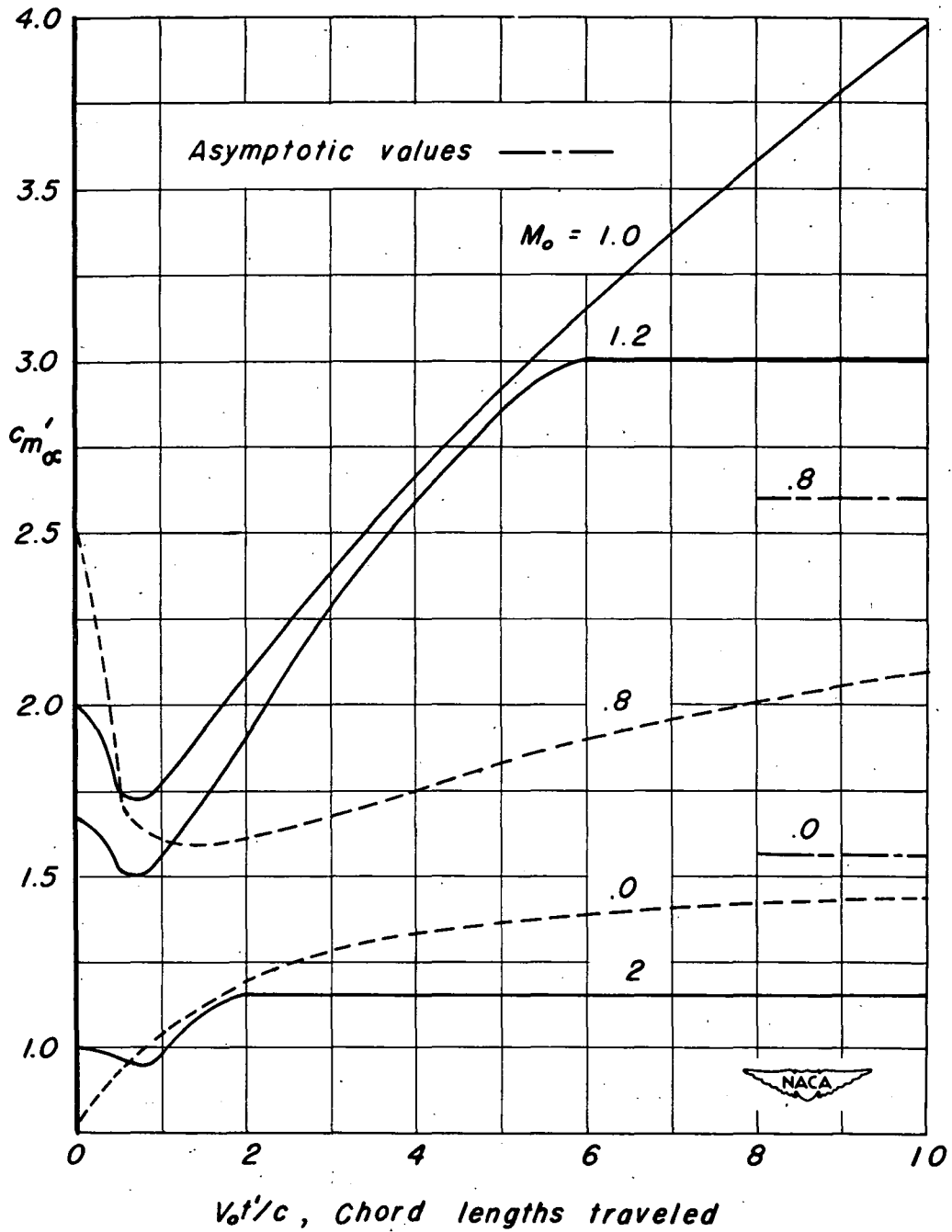
$$M_0 = 0.8$$

t_0	$\frac{\beta}{2\pi} c_{l\alpha}$	$\frac{2\beta}{3\pi} c_{lq}$	$\frac{2\beta}{\pi} c_{m\alpha}$	$\frac{2\beta}{\pi} c_{mq}$
0	0.478	0.318	-0.955	-0.637
.1	.468	.314	-.931	-.618
.2	.458	.312	-.898	-.601
.3	.449	.313	-.857	-.587
.4	.439	.317	-.805	-.578
.5	.430	.325	-.745	-.575
.6	.423	.336	-.689	-.580
.8	.423	.359	-.639	-.600
1.0	.442	.383	-.621	-.620
1.5	.479	.438	-.608	-.664
2.0	.515	.484	-.613	-.694
2.5	.542	.525	-.619	-.716
3.0	.574	.558	-.625	-.727
3.5	.599	.586	-.635	-.735
4.0	.619	.610	-.645	-.740
4.5	.637	.630	-.658	-.747
5.0	.652	.645	-.671	-.755
6.0	.678	.672	-.696	-.773
7.0	.701	.696	-.718	-.790
8.0	.722	.717	-.737	-.804
9	.740	.736	-.754	-.817
10	.757	.752	-.769	-.828
15	.818	.815	-.827	-.871
20	.858	.855	-.865	-.899
25	.885	.883	-.890	-.918
30	.904	.903	-.908	-.932
40	.929	.928	-.932	-.949
50	.945	.944	-.947	-.961
60	.955	.955	-.957	-.968
80	.968	.968	-.969	-.977
100	.976	.975	-.976	-.982
∞	1.000	1.000	-1.000	-1.000



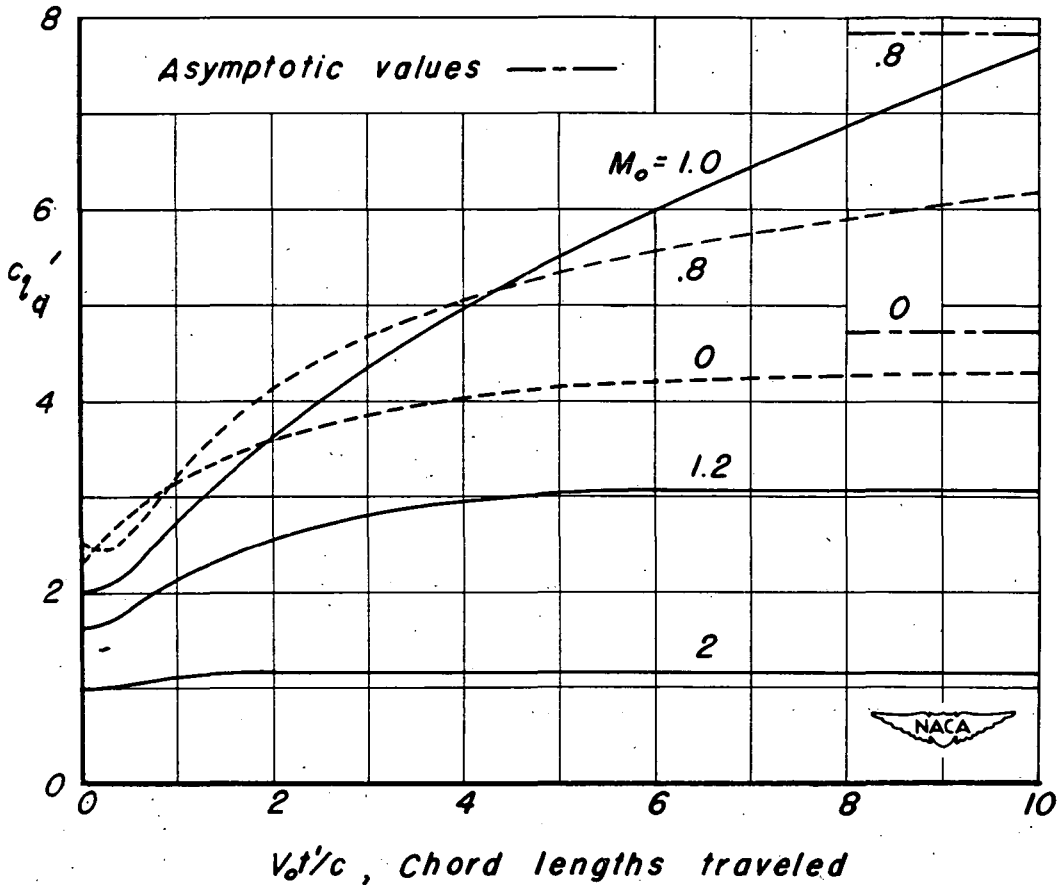
(a) Lift on a sinking wing.

Figure 1.- Variation of two-dimensional indicial lift and pitching-moment coefficients with chord lengths traveled for several Mach numbers.



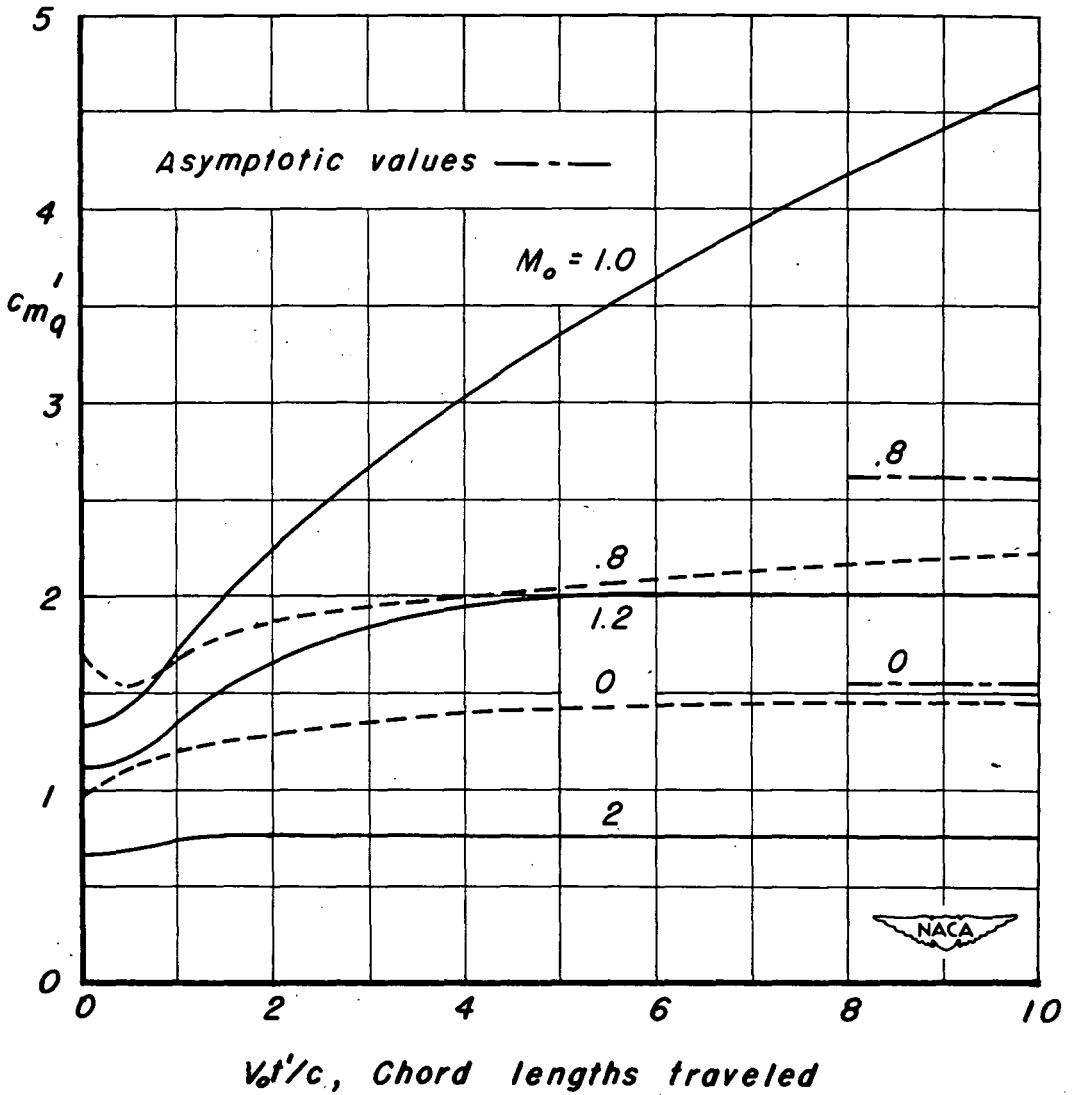
(b) Pitching moment (about leading edge) on a sinking wing.

Figure 1. - Continued.



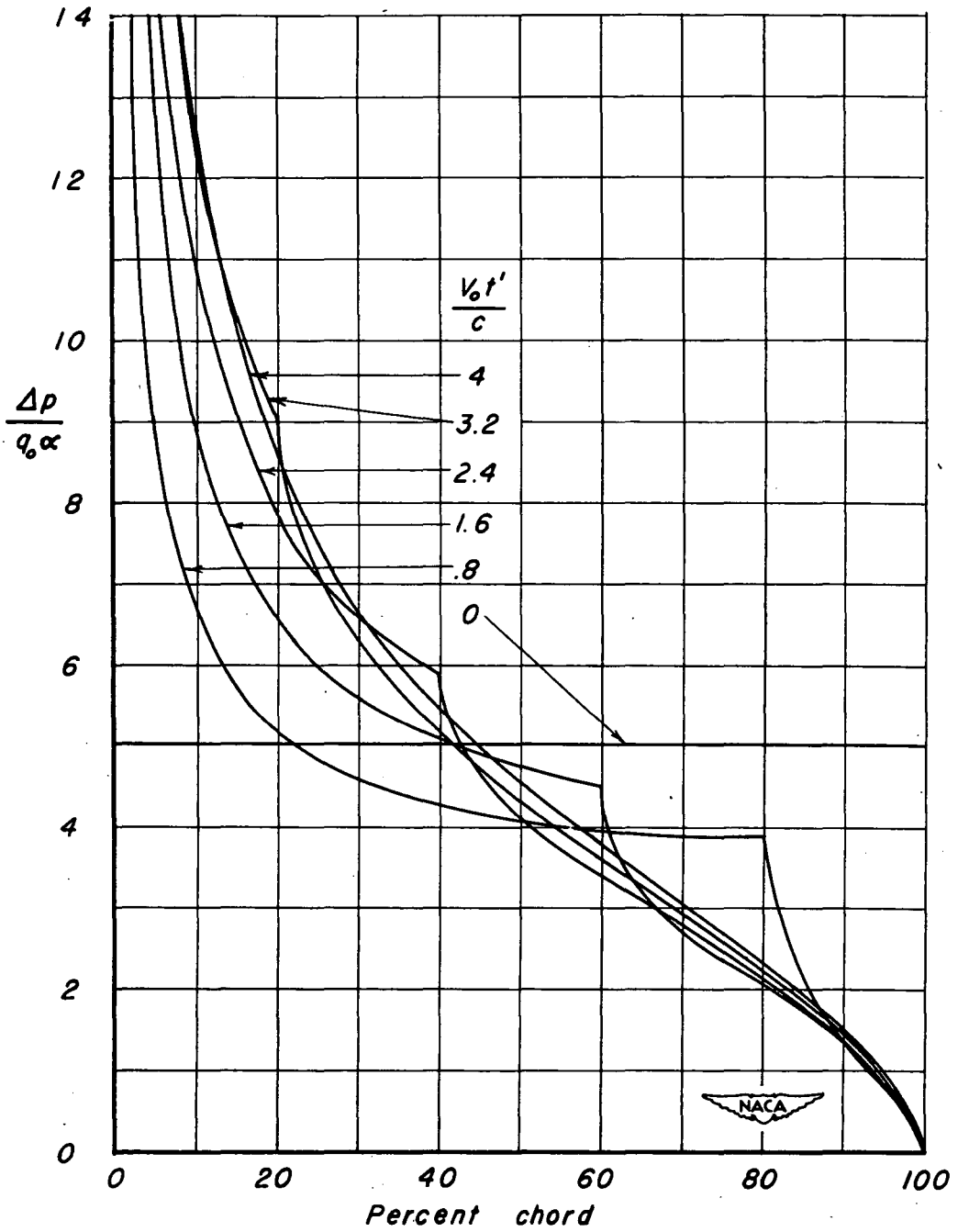
(c) Lift on a wing pitching about its leading edge.

Figure 1. - Continued.



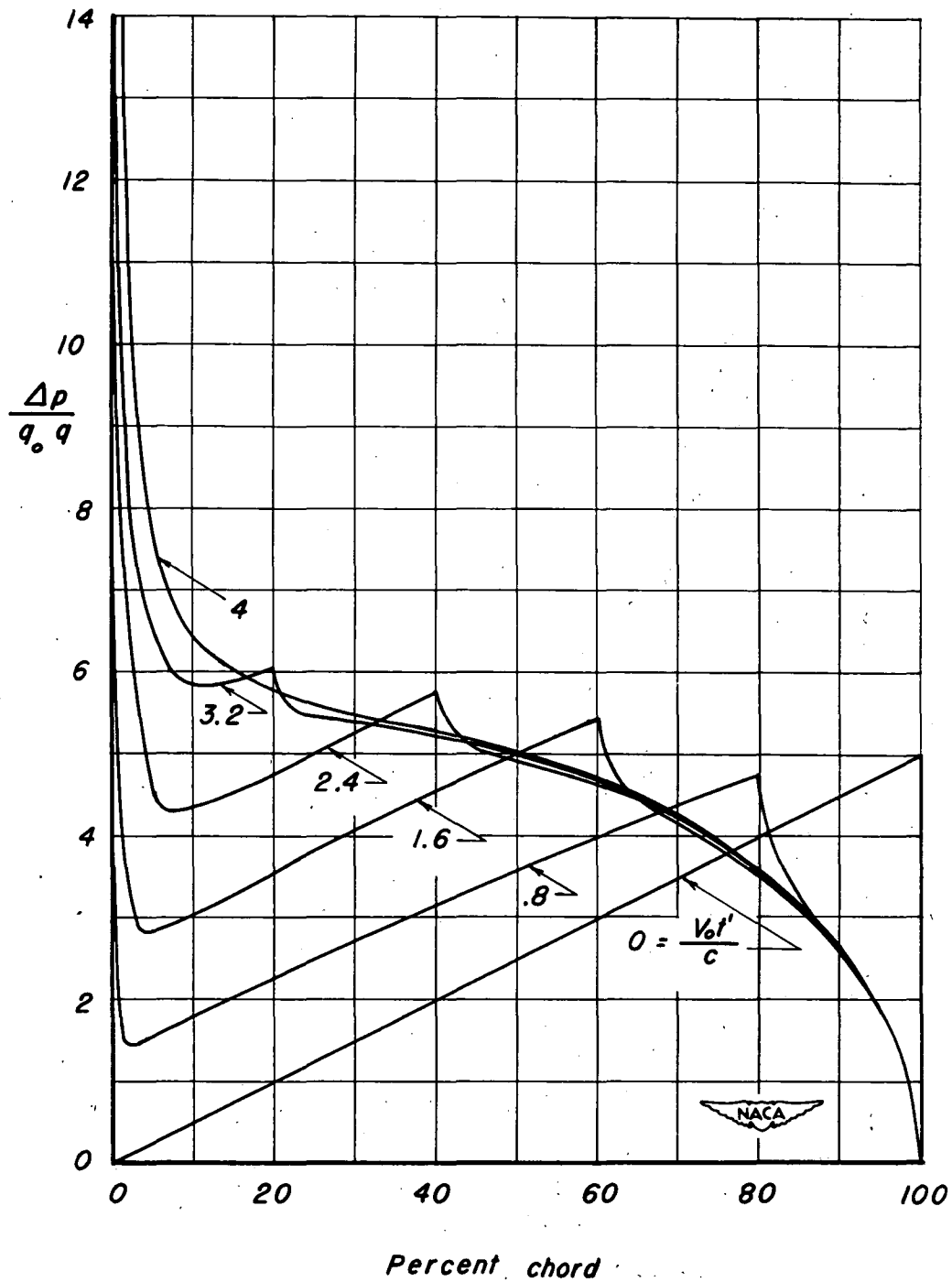
(d) Pitching moment (about leading edge) on a wing pitching about its leading edge.

Figure 1. - Concluded.



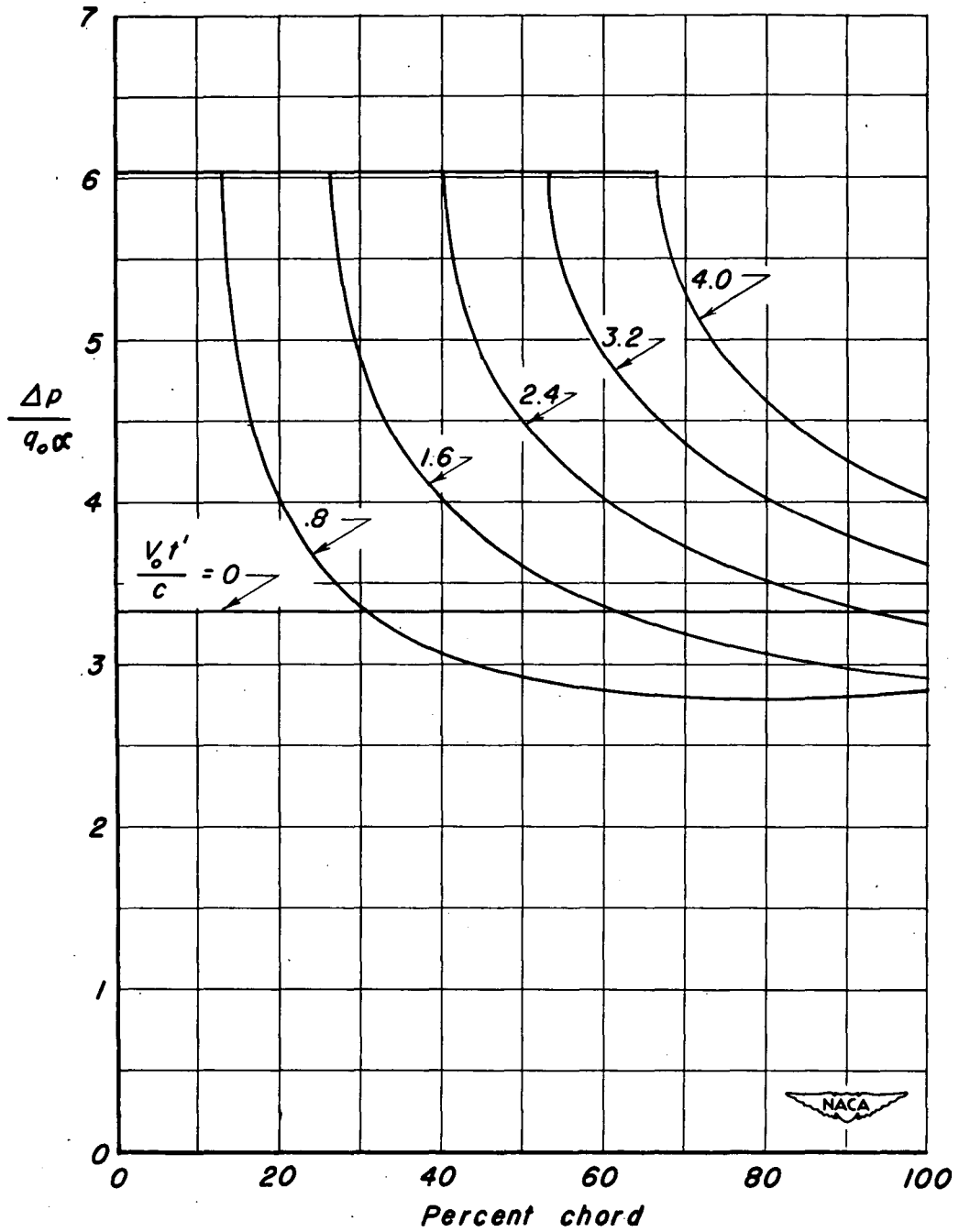
(a) Sinking wing.

Figure 2.- Variation of two-dimensional load distribution with percent chord for a Mach number equal to 0.8.



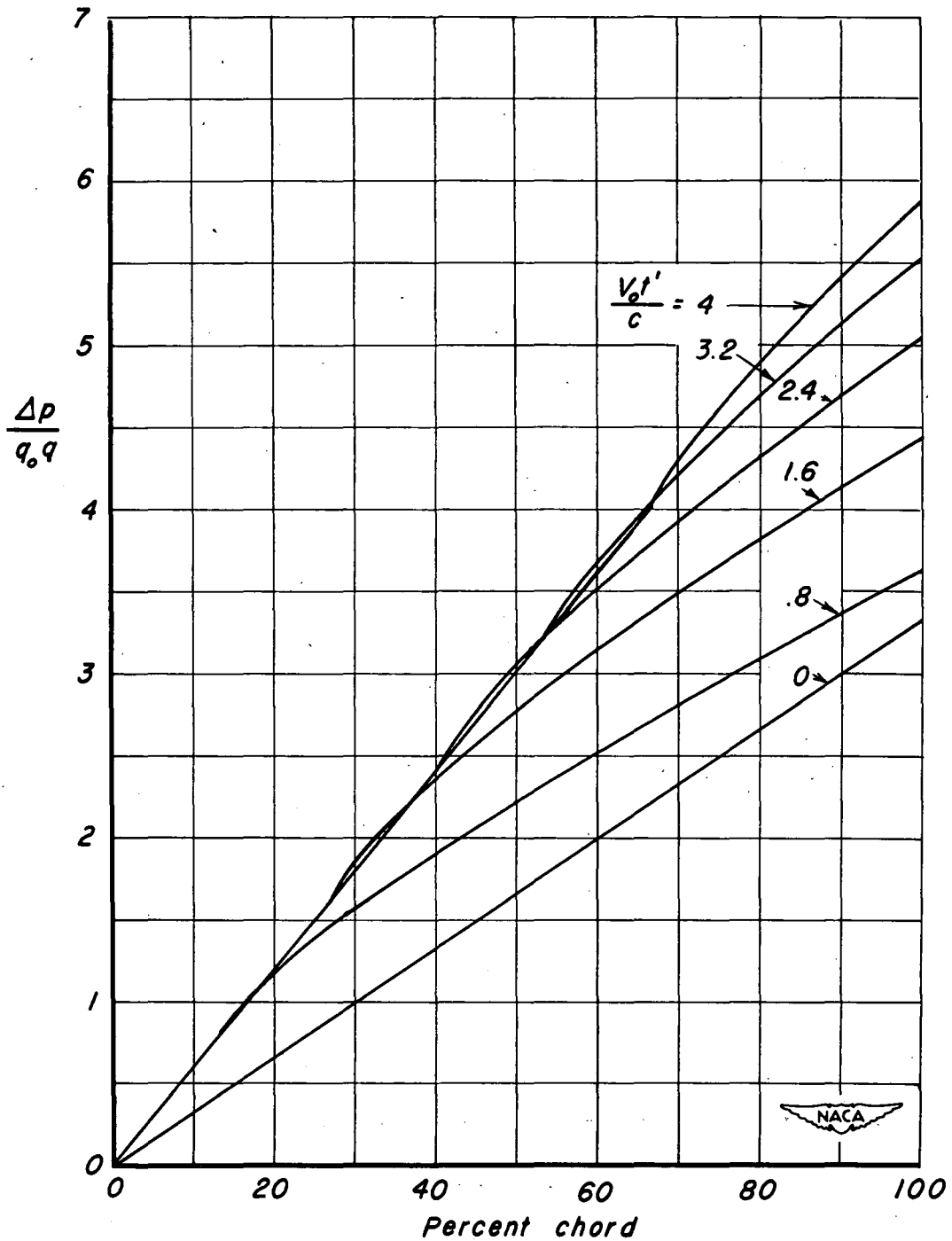
(b) Wing pitching about its leading edge.

Figure 2. - Concluded.



(a) Sinking wing.

Figure 3. - Variation of two-dimensional indicial load distribution with percent chord for a Mach number equal to 1.2.



(b) Wing pitching about its leading edge.

Figure 3. - Concluded.